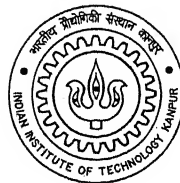


Distortional Buckling in Monosymmetric I-Beams

A Thesis submitted
in Partial Fulfillment of the Requirement
for the Degree of
Master of Technology

by

Avik Samanta



to the

Department of Civil Engineering
Indian Institute of Technology Kanpur

June, 2005

TH
CE/2005/W
Sa 42d

13 OCT 2005 / CE

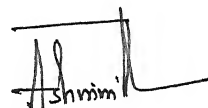
पुष्पोत्तम मणीनाथ केवकर पुस्तकालय
भारतीय ... लेखिका संस्थान कानपुर
अवधि क्र० **153054**



A153054

CERTIFICATE

This is certified that the work contained in this thesis entitled "*Distortional Buckling in Monosymmetric I-Beams*", by Mr. Avik Samanta (Y3103012), has been carried out under my supervision and that this work has not been submitted elsewhere for a degree.

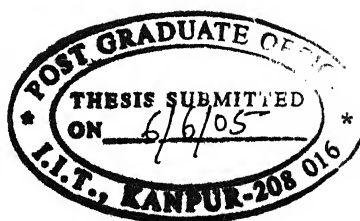
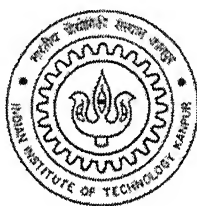


(Ashwini Kumar)

Professor

Department of Civil Engineering
Indian Institute of Technology Kanpur
Kanpur-208016

June, 2005



ABSTRACT

The present investigation deals with distortional buckling in three types of monosymmetric I-beam: (i) simply supported, (ii) propped cantilever, and (iii) braced-cantilever under three types of load: a point load, a uniformly distributed load and a uniform moment. For the first two types of load, both the top flange and the bottom flange load positions are considered. ABAQUS is used in the present investigation. It is found that for comparatively short beams the buckling may be governed by distortion of the web. For the first two types of beam, the moment modification factors are calculated based on the present analysis, which accounts for the distortion of the web, and these are compared with those based on SSRC Guidelines that are based on the lateral-torsional buckling analysis. It is seen that the provisions in SSRC Guidelines may seriously overestimate the critical load for relatively short span beams. For braced cantilever beams, the effect of different kinds of bracing and their position along the length of the beam is investigated. This investigation also gives a comparison of relevant code specifications for the lateral-torsional buckling analysis of monosymmetric I-beams.

Dedicated
To
My Parents

I would first like to thank my advisor, Dr Ashwini Kumar, for his guidance, concern, availability, understanding, and patience. He was always willing to lend a helping hand when I came across any trouble, whether they are associated with academics or life in general. Dr. Kumar perhaps unknowingly passed on to me many lessons that I will carry with me the rest of my life.

I would like to thank my family and friends for their constant support and understanding. To my parents, for their advice. To Dhiraj, Surajit and Manas for providing the much needed relief outside of work. I could not have asked for better friends, without you guys the road would have been much rockier. My association with the various individuals at IIT Kanpur has made my campus-stay pleasant, and I will always cherish the moments I spent with them.

Avik Samanta

CERTIFICATE	i
ABSTRACT	ii
ACKNOWLEDGEMENT	iv
TABLE OF CONTENTS	v
LIST OF FIGURES	vii
LIST OF TABLES.....	xii
LIST OF SYMBOLS.....	xiii

CHAPTER 1: INTRODUCTION

1.1 Stability	1
1.2 Buckling in Beams	1
1.3 Literature Review.....	3
1.4 Present Investigation	6

CHAPTER 2: CODE SPECIFICATIONS

2.1 IS: 800 (1984) Specifications	7
2.2 Revised IS: 800 (Draft) Specifications.....	8
2.3 LRFD Specifications	9
2.4 SSRC Guidelines	10
2.5 Comparison of Different Specifications.....	11

CHAPTER 3: SIMPLY-SUPPORTED BEAMS

3.1 Introduction	19
3.2 Moment Capacities under Flexural-torsional Buckling	21
3.2.1 Uniform Moment	21
3.2.2 Central Point Load	22
3.2.3 Uniformly Distributed Load	22
3.3 Present Investigation	23

3.4 Buckling Loads	24
3.5 Moment Modification Factors	30
3.6 Concluding Remarks	33

CHAPTER 4: PROPPED-CANTILEVER BEAMS: REVERSE-CURVATURE BENDING

4.1 Introduction	34
4.2 Present Investigation	35
4.3 Results	36
4.4 Moment Modification Factors	41
4.5 Concluding Remarks	46

CHAPTER 5: BRACED-CANTILEVER BEAMS

5.1 Introduction	47
5.2 Present Study	48
5.3 Comparison with Results of Kitipornchai et al (1984, 1987)	49
5.4 Buckling Loads	51
5.5 Comparison with SSRC Guidelines	64
5.6 Concluding Remarks	65

CHAPTER 6: SUMMARY AND CONCLUSIONS

6.1 Summary.....	67
6.2 Conclusions.....	68

REFERENCES	70
-------------------------	-----------

<u>Figure</u>	<u>Page No.</u>
Fig. 1.1	Lateral Buckling2
Fig. 1.2	Local Buckling (of web)2
Fig. 1.3	Distortional Buckling3
Fig. 2.1	Beam Cross-section12
Fig 2.2	Comparison of Critical Bending Stress, f_{cb} : <i>Uniform moment</i> ($\rho = 0.9, 0.5, 0.1$)14
Fig 2.3a	Comparison of Critical Bending Stress, f_{cb} : <i>Point Load at top flange</i> ($\rho = 0.9, 0.5, 0.1$)15
Fig 2.3b	Comparison of Critical Bending Stress, f_{cb} : <i>Point Load at bottom flange</i> ($\rho = 0.9, 0.5, 0.1$)16
Fig 2.4a	Comparison of Critical Bending Stress, f_{cb} : <i>UDL at top flange</i> ($\rho = 0.9, 0.5, 0.1$)17
Fig 2.4b	Comparison of Critical Bending Stress, f_{cb} : <i>UDL at bottom flange</i> ($\rho = 0.9, 0.5, 0.1$)18
Fig 3.1	Load Cases Considered19
Fig. 3.2	Beam Cross-section20
Fig. 3.3a	Variation in Buckling Loads: Point Load at Top Flange25
Fig. 3.3b	Variation in Buckling Loads: Point Load at Bottom Flange26
Fig. 3.4a	Variation in Buckling Loads: UDL at Top Flange26
Fig. 3.4b	Variation in Buckling Loads: UDL at Bottom Flange27
Fig. 3.5	Variation in Buckling Loads: Uniform Moment27
Fig. 3.6	Buckled Shape in Simply Supported Beam ($L/h = 4$): <i>Point Load at Mid Span</i>28
Fig. 3.7	Buckled Shape in Simply Supported Beam ($L/h = 8$): <i>Point Load at Mid Span</i>29
Fig. 3.8a	Comparison of Moment Modification Factors C_b with ρ : <i>Point Load at Top Flange</i>31

Fig. 3.8b	Comparison of Moment Modification Factors C_b with ρ : <i>Point Load at Bottom Flange</i>	31
Fig. 3.9a	Comparison of Moment Modification Factors C_b with ρ : <i>UDL at Top Flange</i>	32
Fig. 3.9b	Comparison of Moment Modification Factors C_b with ρ : <i>UDL at Bottom Flange</i>	32
Fig. 4.1	Load Cases Considered	35
Fig. 4.2a	Variation in Distortional Buckling Loads: <i>Point Load at Top Flange</i>	37
Fig. 4.2b	Variation in Distortional Buckling Loads: <i>Point Load at Bottom Flange</i>	38
Fig. 4.3a	Variation in Distortional Buckling Loads: <i>UDL at Top Flange</i>	38
Fig. 4.3b	Variation in Distortional Buckling Loads: <i>UDL at Bottom Flange</i>	39
Fig. 4.4	Buckled Shape of a Propped-Cantilever Beam ($L/h=4$): Point Load at Mid Span	40
Fig. 4.5	Buckled Shape of a Propped-Cantilever Beam ($L/h=10$): Point Load at Mid Span	41
Fig. 4.6	Comparison of Moment Modification Factors C_b with ρ : <i>Point Load at Top Flange</i>	43
Fig. 4.7	Comparison of Moment Modification Factors C_b with ρ : <i>Point Load at Bottom Flange</i>	43
Fig 4.8	Comparison of Moment Modification Factors C_b with ρ : <i>UDL at Top Flange</i>	44
Fig 4.9	Comparison of Moment Modification Factors C_b with ρ : <i>UDL at Bottom Flange</i>	44
Fig 4.10a	Comparison of Moment Modification Factors C_b with ρ : <i>Point Load at Top Flange ($L/h=12$)</i>	45

Fig 4.10b	Comparison of Moment Modification Factors C_b with ρ : <i>Point Load at Top Flange</i> ($L/h=6$)45
Fig 4.11a	Comparison of Moment Modification Factors C_b with ρ : <i>Point Load at Bottom Flange</i> ($L/h=12$)45
Fig 4.11b	Comparison of Moment Modification Factors C_b with ρ : <i>Point Load at Bottom Flange</i> ($L/h=6$)45
Fig. 5.1	Load Cases Considered49
Fig. 5.2	Types of Bracing49
Fig. 5.3	Buckled Shape in Cantilever Beam ($L/h = 2$): Point Load at Free End51
Fig. 5.4	Buckled Shape in Cantilever Beam ($L/h = 5.33$): Point Load at Free End52
Fig. 5.5	Variations in Buckling Loads with Location of Different Types of Lateral Brace: <i>Point Load at Top Flange</i> ($L/h=2, \rho=0.5$)55
Fig. 5.6	Variations in Buckling Loads with Location of Different Types of Lateral Brace: <i>UDL at Top Flange</i> ($L/h=2, \rho=0.5$)55
Fig. 5.7	Variations in Buckling Loads with Location of Different Types of Lateral Brace: <i>Point Load at Bottom Flange</i> ($L/h=2, \rho=0.5$)55
Fig. 5.8	Variations in Buckling Loads with Location of Different Types of Lateral Brace: <i>UDL at Bottom Flange</i> ($L/h=2, \rho=0.5$)56
Fig. 5.9	Variations in Buckling Loads with Location of Different Types of Lateral Brace: <i>Point Load at Top Flange</i> ($L/h=5.33, \rho=0.5$)56
Fig. 5.10	Variations in Buckling Loads with Location of Different Types of Lateral Brace:

	<i>UDL at Top Flange</i> ($L/h=5.33$, $\rho=0.5$)	56
Fig. 5.11	Variations in Buckling Loads with Location of Different Types of Lateral Brace:	
	<i>Point Load at Bottom Flange</i> ($L/h=5.33$, $\rho=0.5$)	57
Fig. 5.12	Variations in Buckling Loads with Location of Different Types of Lateral Brace:	
	<i>UDL at Bottom Flange</i> ($L/h=5.33$, $\rho=0.5$)	57
Fig. 5.13	Variations in Buckling Loads with Location of Different Types of Lateral Brace:	
	<i>End Moment</i> ($L/h=2$, $\rho=0.5$)	57
Fig. 5.14	Variations in Buckling Loads with Location of Different Types of Lateral Brace:	
	<i>End Moment</i> ($L/h=5.33$, $\rho=0.5$)	58
Fig. 5.15	Variations in Buckling Loads with Location of Lateral Brace:	
	<i>Point Load at Top Flange, <u>Bracing at Top Flange</u></i> ($L=2m$)	58
Fig. 5.16	Variations in Buckling Loads with Location of Lateral Brace:	
	<i>UDL at Top Flange, <u>Bracing at Top Flange</u></i> ($L=2m$)	58
Fig. 5.17	Variations in Buckling Loads with Location of Lateral Brace:	
	<i>Point Load at Bottom Flange, <u>Bracing at Top Flange</u></i> ($L=2m$)	59
Fig. 5.18	Variations in Buckling Loads with Location of Lateral Brace:	
	<i>UDL at Bottom Flange, <u>Bracing at Top Flange</u></i> ($L=2m$)	59
Fig. 5.19	Variations in Buckling Loads with Location of Lateral Brace:	
	<i>Point Load at Top Flange, <u>Bracing at Bottom Flange</u></i> ($L=2m$).....	59
Fig. 5.20	Variations in Buckling Loads with Location of Lateral Brace:	
	<i>UDL at Top Flange, <u>Bracing at Bottom Flange</u></i> ($L=2m$)	60
Fig. 5.21	Variations in Buckling Loads with Location of Lateral Brace:	
	<i>Point Load at Bottom Flange,</i> <i><u>Bracing at Bottom Flange</u></i> ($L=2m$)	60
Fig. 5.22	Variations in Buckling Loads with Location of Lateral Brace:	
	<i>UDL at Bottom Flange, <u>Bracing at Bottom Flange</u></i> ($L=2m$)	60

Fig. 5.23	Variations in Buckling Loads with Location of Lateral Brace: <i>Point Load at Top Flange,</i> <u>Bracing at Top & Bottom Flange (L=2m)</u>61
Fig. 5.24	Variations in Buckling Loads with Location of Lateral Brace: <i>UDL at Top Flange, Bracing at Top & Bottom Flange (L=2m)</i>61
Fig. 5.25	Variations in Buckling Loads with Location of Lateral Brace: <i>Point Load at Bottom Flange,</i> <u>Bracing at Top & Bottom Flange (L=2m)</u>61
Fig. 5.26	Variations in Buckling Loads with Location of Lateral Brace: <i>UDL at Bottom Flange, Bracing at Top & Bottom Flange (L=2m)</i>62
Fig. 5.27	Variations in Buckling Loads with Location of Lateral Brace: <i>End Moment, Bracing at Top Flange (L=2m)</i>62
Fig. 5.28	Variations in Buckling Loads with Location of Lateral Brace: <i>End Moment, Bracing at Bottom Flange (L=2m)</i>63
Fig. 5.29	Variations in Buckling Loads with Location of Lateral Brace: <i>End Moment, Bracing at Top & Bottom Flange (L=2m)</i>63

LIST OF TABLES

<u>Table</u>		<u>Page No.</u>
Table 2.1	Beam sections	12
Table 4.1	Beam sections	36
Table 5.1	Table for Effective Length Factors (K_{ef})	47
Table 5.2	Comparison of Results.....	50
Table 5.3	Comparison with SSRC Guidelines for $L=2m$ ($L/h=3.33$)	64

LIST OF SYMBOLS

a	distance of the shear center S from the top flange shear center
B	lateral bracing at the bottom flange of beam
B_T, B_B	top, bottom flange width
β_x	monosymmetric property
C_b	moment modification factor
C	centroid of the cross-section
D	overall depth of the beam
E	Young's modulus of elasticity
FB	full brace (lateral & rotational brace at both top and bottom flanges)
f_y	yield stress of steel
f_{cb}	elastic critical stress in bending
ϕ_T, ϕ_B	angle of twist at top, bottom flange
G	shear modulus of elasticity
ξ	distance of the load position from the mid-height between the flange centroids
γ_c	non-dimensional elastic moment
ν	Poisson's ratio
h	distance between flange centroids
h_s	distance between shear center of the two flanges of the cross-section
I_x	moment of inertia about x-axis
I_y	moment of inertia about y-axis
I_{y-top}	moment of inertia of the top flange about y-axis
I_{YT}	second moment of area about the section y-axis of the top flange
I_{YB}	second moment of area about the section y-axis of the bottom flange
I_w	warping section constant
J	torsional section constant
L, l	length of the beam
M	uniform moment

M_{\max}	absolute value of the unbraced moment in the unbraced segment
M_A	absolute values of the moments at the quarter point in the braced segment
M_B	absolute values of the moments at the center point in the braced segment
M_C	absolute values of the moments at the three-quarter point in the braced segment
M_{or}	elastic critical moment of a cantilever beam under uniform bending
P	point load
q	uniformly distributed load per unit length
r_y	radius of gyration of the section about y-axis
θ	angle of twist of the web
ρ	measure of beam mono-symmetry
S	shear center of the cross-section
T_C	mean thickness of the compression flange
T	lateral bracing at the top flange of beam section
TB	lateral bracing at both the top & bottom flange of the beam
t	web thickness
T_T, T_B	top, bottom flange thickness
u_T, u_B	lateral displacements of top, bottom flange
σ_{bc}	maximum permissible stress in bending compression
\bar{y}	distance of the centroid C from the top flange shear center

INTRODUCTION

1.1 Stability

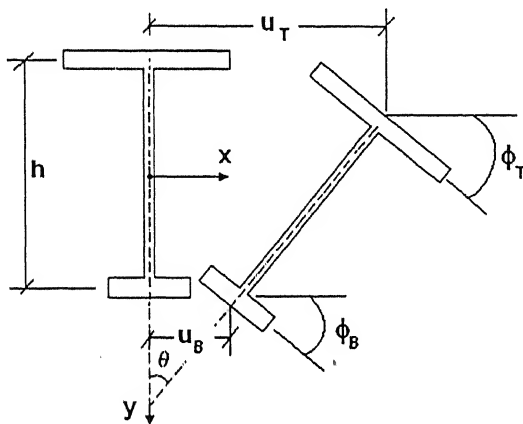
The stability of a structure essentially means the stability of its equilibrium configuration or state. In practical sense, an equilibrium state of a structure or a system is said to be stable if accidental forces, shocks, vibrations, imperfections or other probable irregularities do not cause the system to depart excessively from that state. In mathematical sense, the stability is usually interpreted to mean that infinitesimal disturbances will cause only infinitesimal departure from the given equilibrium configuration.

While designing structures, care should be taken so that the 'failure' does not occur in the structure. This 'failure' may be of two kinds: (i) material failure (ii) geometric or form failure. In the first case, stresses in the material due to loads in the structure exceed certain safe limits, which essentially causes cracks and lead to failure. In the second case, stresses in the material due to loads in the structure do not exceed safe limits but excessive deformation may take place in the structure and the structure may not keep up the form in which it is designed. The loss of stability due to tensile loads falls in the first category, whereas the loss of stability under compressive loads is usually termed structural (or geometric or form) instability, commonly known as buckling.

1.2 Buckling in Beams

Consider the case of beams in which the applied loads produce principally the bending moment and the shear force while the axial force remains negligibly small. Most of the beams are designed to carry loads which cause bending about the major principal axis of the cross-section, which is called the in-plane bending. Beams are assumed to be deflected only in the stiffer principal plane here. In case of I-beams, they do not have sufficient lateral stiffness and as they are open sections, they are not very efficient in resisting torsion as well. So, even though the in-plane bending does not introduce torsion intentionally, it exists from the very beginning of loading due to unavoidable initial

imperfections in the beam geometry and due to the unintentional small eccentricity of loads. This may cause the beam to bend laterally (out of the plane of loading) and the load at which this happens may be substantially less than the in-plane load carrying capacity of the beam. This phenomenon is known as lateral-torsional buckling. The out-of plane deformation becomes magnified to the extent that they terminate the usefulness of the beam. Here, the compression flange becomes unstable. This kind of buckling is considered to involve general lateral deflection and twist along the member length without any change in the cross-sectional shape (Fig. 1.1).

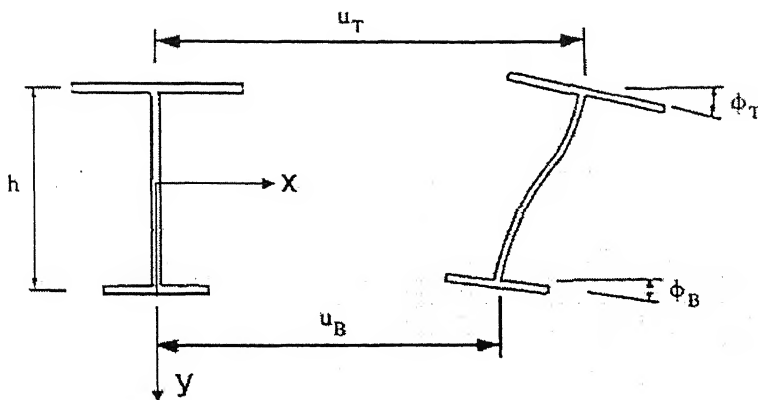


Lateral-torsional Buckling
Fig. 1.1



Local Buckling (of Web)
Fig. 1.2

Another mode of buckling is one in which an element of the member, such as the compression flange or web, is considered to buckle locally over a short length of the member with local changes in cross sectional shapes (Fig. 1.2). Usually in designing steel beam members either the effect of lateral-torsional buckling or the local buckling is taken into account. However, it is very well recognized that these two modes of member buckling may also interact. This particular mode of buckling is called distortional buckling (Fig. 1.3). In this mode, the web distorts and allows flanges to deflect laterally with comparatively little twist, and thus reduces the effective torsional resistance of the member. This is more significant in plate girders with slender, un-stiffened webs than in I-sections with comparatively stocky webs.



Distortional Buckling
Fig. 1.3

1.3 Literature review

The literature review reveals that a large number of investigations are available which deal with lateral-torsional buckling of I-beams under different load cases. The basic treatment of buckling of I-beams having doubly-symmetric cross-section is available in almost all books on stability of structures and can be seen in, for example, Timoshenko and Gere (1961), Chajes (1974). Some preliminary studies on buckling of monosymmetric I-beams are due to Winter (1941), Goodier (1941) and Hill (1942) and, later on, by Petterson (1951), Kerensky et al (1956) and O'Conner (1964).

In the design of mono-symmetric I-beams one of the initial difficulties was how to express the key section properties required for calculating the elastic critical moment. There was no uniformity in the expressions derived in different investigations and the resulting expression turned out to be cumbersome in applications. Kitipornchai and Trahair (1980) overcame this difficulty by proposing simple expressions to define section properties and derived an expression for the elastic critical buckling stress for the case of constant moment. Using the finite integral method and the Rayleigh-Ritz energy approach, Kitipornchai et al (1986) investigated buckling of mono-symmetric I-beams under moment gradient and proposed an expression for the non-dimensional elastic moment γ_c . Wang and Kitipornchai (1986) did a similar investigation and obtained approximate expressions for non-dimensional elastic moment γ_c at buckling under

different transverse load cases. Helwig et al (1997) suggested expressions for moment modification factors to cover general load cases; when this modification factor is applied to the moment capacity of the beam for a uniform moment case, it yields the critical moment for a particular load case. Some of these research findings have been incorporated for stability design considerations in beams by the Structural Stability Research Council (hereafter, referred as SSRC Guidelines) which can be found in Galambos (1998).

During last twenty-five years some researchers have investigated beam buckling problems taking into account the distortion of web. Hancock et al (1980) have shown that the web distortion allows flanges to deflect laterally with comparatively little twist, reduces the effective torsional resistance of the member and consequently reduces the resistance to flexural-torsional buckling. An approximate energy method was used to analyze the effect of web distortion on elastic flexural-torsional buckling. Nonlinear elasticity theory was used by Bradford and Trahair (1981) to develop a finite element method for investigating the elastic distortional buckling of I-beams under end moments. The web was assumed to be flexible and distorted as a cubic curve in the plane of the cross-section. It was shown that the effect of web distortion on flexural-torsional buckling was more for short and of intermediate length beams in which the end-displacements and rotations of flanges were allowed. Bradford has published a series of papers taking into account the distortion of webs in I- and T-section beams. Using finite element method, Bradford (1985) studied the effect of web slenderness on a mono-symmetric I-beam both under a uniform moment and in the presence of moment gradient. A design equation was developed to determine the distortional buckling stress. An approximate energy method was developed by Bradford (1988) to investigate distortional buckling in I-beams having continuous restraints. Later this investigation was extended to include T-section beams (Bradford, 1990). Using nonlinear elasticity theory, Ma & Hughes (1996) developed an energy method to analyze the distortional buckling in mono-symmetric I-beams. It was shown that, for doubly symmetric I-section beams, the disparity between distortional and classical critical loads increases as the ratio h/L increases. Recently, Loong-Hon Ng and Ronagh (2004) developed a mathematical model using Fourier series to study the effect of distortional buckling in beams.

Very few studies are available related to lateral-torsional buckling in I beams under reverse curvature bending. The most notable work is that of Helwig et al (1997) who investigated the buckling behaviour of fixed-end beams and propped cantilever beams with monosymmetric I-section, in reverse-curvature bending. Based on the investigation some expressions were suggested for the moment modification factor in such beams. These expressions, with some modifications, have been included in the specifications given by SSRC Guidelines (1998) for the design of beams.

Timoshenko and Gere (1961) obtained the elastic critical moment for cantilever beams under a uniform moment. Nethercot (1983) suggested a simple effective length method for calculating the critical moment for various restraint conditions at the tip and at the root of the cantilever. Kiripornchai et al (1984) investigated the elastic flexural-torsional buckling behaviour of cantilever I-beams using the finite integral method. Considering two load cases, a point load and a uniformly distributed load, they examined the effects of beam parameters, the load height, the location and the level of restraint along the beam on the buckling load. They considered translational, rotational and full restraint conditions along the cantilever. Based on some experiments on aluminium cantilever I-beams, it was shown that the experimental buckling loads were generally lower than theoretical predictions. Wang et al (1987) calculated the buckling capacity of monosymmetric cantilever beams using Timoshenko energy approach. They considered a concentrated load and a uniform moment and studied the effect of translational, rotational and full restraint conditions on the buckling load.

Investigations that take into account distortional buckling in cantilever are very few. Johnson and Will (1974) demonstrated that a doubly-symmetric cantilever with a stocky web could buckle in a distortional mode at a load somewhat lower than that which would cause lateral buckling. Bradford (1992) employed finite element method of analysis which used line elements for the beam discretization and allowed cross-sectional distortion. A case of point load at the tip was considered to show the influence of cross-sectional proportions and the load height on the critical load. The analysis showed that the elastic distortional buckling load may be well below the elastic lateral buckling load and a large reduction in the buckling load may occur due to web distortion when the beam is short, web is very slender and the load is positioned away from the shear centre.

Bradford (1999) extended the study of distortional buckling to T-section cantilever beams for three load cases: a point load at free end, a uniformly distributed load and a uniform moment. Influence of cross-sectional proportions and the position of brace along the cantilever on the critical load was examined. It was shown that in all cases when web is slender, the distortional buckling load is somewhat less than the lateral torsional buckling load, and that the effect of distortion is significantly high for short length members.

1.4 Present Investigation

From the literature review it is observed that in dealing with the problem of buckling in beams, following issues/aspects have been under consideration.

- Type of buckling : Lateral torsional, distortional
- Type of beam : Simply supported, cantilever with/without bracings, propped cantilever
- Type of beam-section: Doubly symmetric, monosymmetric I-section
- Type of load : Point load, uniformly distributed load, uniform moment, moment gradient

While a large number of investigations are available in respect of lateral torsional buckling of beams, the available literature on distortional buckling of short span beams with monosymmetric I-sections is limited. Hence the present investigation is aimed at the detailed study of distortional buckling in short span simply supported, propped cantilever, braced cantilever beams using ABAQUS. Whenever possible, the results are compared with existing codal design specifications.

The present investigation is as under:

Chapter 2: Review of code provisions

Chapter 3: Distortional buckling of simply-supported monosymmetric I-beams under three load cases (point load, udl, uniform moment)

Chapter 4: Distortional buckling of propped cantilevers under double curvature bending

Chapter 5: Distortional buckling of cantilever beams with different kinds of bracings, under three load cases.

Chapter 6: Summary and conclusions.

CODE SPECIFICATIONS

In this chapter specifications related to buckling in beams available in different codes are presented. Various specifications are then compared by considering I-beams with varying degree of monosymmetry.

2.1 IS: 800 (1984) Specifications

IS: 800 (1984) uses the following Merchant-Rankine formula to get the maximum permissible bending compressive stress σ_{bc} in designing I-beams:

$$\sigma_{bc} = \frac{0.66 f_{cb} f_y}{[(f_{cb})^n + (f_y)^n]^{1/n}} \quad (2.1)$$

where f_y is the yield stress of steel; n is the imperfection factor ($=1.4$ for welded or riveted members); f_{cb} is the elastic critical stress in bending. To determine f_{cb} , the code proposes the following formula or suggests the use of elastic flexural-torsional buckling analysis:

$$f_{cb} = k_1 (X + k_2 Y) \frac{c_2}{c_1} \quad (2.2)$$

where $X = Y \sqrt{\left[1 + \frac{1}{20} \left(\frac{l T_c}{r_y D} \right)^2 \right]}$ MPa (2.3)

$$Y = \frac{26.5 X 10^5}{(l/r_y)^2} \text{ MPa} \quad (2.4)$$

k_1 = a coefficient to allow for the reduction in thickness or breadth of flanges between points of effective lateral restraint, and depends on ψ , the ratio of the total area of both flanges at the point of least bending moment to the corresponding area at the point of greatest bending moment between such points of restraint.

D = overall depth of the beam;

l = effective length of the compression flange;

r_y = radius of gyration of the section about its axis of minimum strength (y-y axis);

T_C = mean thickness of the compression flange, is equal to the area of horizontal portion of flange divided by width;

k_2 = a coefficient to allow for the inequality of flanges, and depends on ω , the ratio of the moment of inertia of the compression flange alone to that of the sum of the moments of inertia of the flanges, each calculated about it's own axis parallel to the y-y axis of the girder, at the point of maximum bending moment.

c_1, c_2 = respectively the lesser and greater distances from the section neutral axis to the extreme fibres.

I_y = moment of inertia of the whole section about the axis lying in the plane of bending (axis y-y),

I_x = moment of inertia of the whole section about the axis normal to the plane of bending (x-x axis).

The buckling formula (2.2) is derived by making use of the equation which is obtained for the elastic critical moment of a simply supported, uniform, monosymmetric, I-beam subjected to a constant moment. In actual practice the member loading can be of any type, resulting in various forms of bending moment variations, e. g. a linear moment gradient, or as in the case of a point load at mid-span and a uniformly distributed load. Under these circumstances one is not sure whether it would be correct to use the available expressions in the code. Moreover, the effect of position of load in the beam (e. g. top flange loading, bottom flange loading or shear center loading) has not been taken into account.

2.2 Revised IS: 800 (Draft) Specifications

These specifications are in the draft form only. The revised provisions take into account the effect of different types of load and the load positions. It suggests the following general equation for elastic critical moment for lateral torsional buckling in monosymmetric beams:

$$M_{cr} = c_1 \frac{\pi^2 EI_y}{(KL)^2} \left\{ \left[\left(\frac{k}{k_w} \right)^2 \frac{I_w}{I_y} + \frac{GI_t (KL)^2}{\pi^2 EI_y} + (c_2 y_g - c_3 z_j)^2 \right]^{0.5} - (c_2 y_g - c_3 z_j) \right\} \quad (2.5)$$

where

c_1, c_2, c_3 = factors depending upon the loading and end restraint conditions

k, k_w = effective length factors of the unsupported length accounting for boundary conditions at the end lateral supports. They vary from 0.5 for full fixity (against warping) to 1.0 for free (to warp) case with 0.7 for the case of one end fixed and other end free.

y_g = y distance between the point of the load and the shear centre of the cross-section and is positive when the load is acting towards the shear center from the point of application.

For plane flanges z_j can be calculated by using the following approximation:

$$z_j = 0.8(2\beta_f - 1) h_s / 2.0 \quad (\text{when } \beta_f > 0.5)$$

$$z_j = 1.0(2\beta_f - 1) h_s / 2.0 \quad (\text{when } \beta_f \leq 0.5)$$

in which

h_s = distance between shear center of the two flanges of the cross-section

$$I_t = \sum b_i t_i^3 / 3 \quad \text{for open sections}$$

$$I_w \begin{cases} = (1 - \beta_f) \beta_f I_y h_s^2 & \text{for I sections monosymmetric about weak axis} \\ = 0 & \text{for angle, Tee, narrow rectangular section} \end{cases}$$

$$\beta_f = I_{fc} / (I_{fc} + I_{ft})$$

where I_{fc} , I_{ft} are the moment of inertia of the compression and tension flanges, respectively, about the minor axis of the entire section.

2.3 LRFD Specifications

Most design specifications provide solutions for lateral torsional buckling of beams under a uniform moment. To account for the effect of the variable moment along the unbraced girder length, a factor C_b , called the 'moment modification factor' is applied to solutions for the uniform moment case. Various formulae have been proposed for C_b , but the most commonly used formulae in many design specifications are the following:

$$C_b = 1.75 + 1.05(M_1/M_2) + 0.3(M_1/M_2)^2 \leq 2.3 \quad (2.6a)$$

$$1/C_b = 0.6 - 0.4(M_1/M_2) \leq 2.5 \quad (2.6b)$$

where M_1 , M_2 are the smaller and larger moments at the ends of the unbraced length, respectively. The ratio M_1/M_2 is taken positive for moments causing reverse-curvature bending and negative for moments causing single-curvature bending. These equations should be applied for moment diagrams which are straight within the unbraced segment.

For many practical problems these equations can not be applied. So, to account for moment gradients, the American Institute of Steel Construction's (AISC) *Load and Resistance Factor Design* (LRFD) Specification (1994) has incorporated the following expression for C_b , which is applicable for linear and non-linear moment diagrams:

$$C_b = \frac{12.5M_{\max}}{2.5M_{\max} + 3M_A + 4M_B + 3M_C} \quad (2.7)$$

where M_{\max} is the absolute value of the unbraced moment in the unbraced segment, and M_A , M_B and M_C are the absolute values of the moments at the quarter point, center, and the three-quarter point, respectively, in the braced segment. The American Association of State Highway and Transportation Officials (AASHTO) *LRFD* specification (1994) had included the equation (2.6a) and (2.7) in its specifications while the American Institute of Steel Construction's (AISC) *Load and Resistance Factor Design* (LRFD) *Specification for Structural Steel Buildings* (1999) is using the equation (2.6a), (2.6b) and (2.7).

2.4 SSRC Guidelines

The C_b values given in section 2.3 are intended for doubly symmetric sections with transverse load applied at the mid-height. When the loads are not applied at the mid-height, the effect of the load height needs to be considered. Based on studies by Nethercot & Rockey (1972) and Nethercot (1983) to account for the effect of load height, the SSRC Guidelines (Galambos, 1988) recommended the following equation for C_b :

$$C_b = AB^{2\xi/h} \quad (2.8)$$

In the above equation, ξ is the distance of the load position from the mid-height between the flange centroids and is taken positive downwards. A and B are two variables which depend upon the type of loading and the warping stiffness of the cross section.

For example,

$$\text{Central point load:} \quad A = 1.35 \text{ and } B = 1 - 0.180K^2 + 0.649K$$

$$\text{Uniformly distributed load:} \quad A = 1.12 \text{ and } B = 1 - 0.154K^2 + 0.535K$$

where K is the beam parameter (defined in section 3.2 of Chapter 3).

Later, the SSRC Guidelines (Galambos, 1998) incorporated effects of the load height and the load condition by taking $B=1.4$ and $A = C_b$, as given by equation (2.7), which lead to the following expression for C_b :

$$C_b = \frac{12.5M_{\max}}{2.5M_{\max} + 3M_A + 4M_B + 3M_C} (1.4^{2\xi/h}) \quad (2.9)$$

These SSRC Guidelines (1998) also recommend a method that takes into account the reverse curvature bending due to loads in monosymmetric I-section beams. The following expression for C_b , for beam sections with $0.1 \leq \rho \leq 0.9$, is suggested:

$$C_b = \frac{12.5M_{\max}}{2.5M_{\max} + 3M_A + 4M_B + 3M_C} (1.4^{2\xi/h}) R \quad (2.10)$$

For beams under single curvature bending $R=1$; for beams under reverse curvature between brace points:

$$R = 0.5 + 2\rho^2 \quad (2.11)$$

where
$$\rho = \frac{I_{y-top}}{I_y} \quad (2.12)$$

I_{y-top} = moment of inertia of the top flange about the y-axis,

I_y = moment of inertia of the whole section about the the y-axis.

In the case of a simply supported beam of span L , following results are quickly recovered:

Central point load P ,

$$M_{\max} = PL/4, \quad M_A = M_C = PL/8, \quad M_B = PL/4$$

$$C_b = 0.940, \quad \text{top flange loading } (\xi = -0.5h) \\ = 1.842, \quad \text{bottom flange loading } (\xi = 0.5h)$$

Uniformly distributed load of intensity q ,

$$M_{\max} = qL^2/8, \quad M_A = M_C = 3qL^2/32, \quad M_B = qL^2/8$$

$$C_b = 0.812, \quad \text{top flange loading } (\xi = -0.5h) \\ = 1.591, \quad \text{bottom flange loading } (\xi = 0.5h)$$

2.5 Comparison of Different Specifications

A comparison is made of the elastic critical stress of a simply supported beam for three load cases: a central point load, a uniformly distributed load and a uniform sagging moment. Specifications taken for comparison are: IS: 800 (1984), new IS: 800 (draft) and SSRC Guidelines (1998) [LRFD specifications are not considered because SSRC

Guidelines are modified over LRFD specification]. The beam sections used for the comparison are given in Table 2.1 and notations are shown in Fig. 2.1.

Table 2.1 Beam Sections:

No.	ρ	h (mm)	B_T (mm)	T_T (mm)	B_B (mm)	T_B (mm)	t (mm)
1	0.1	600	100	20	210	20	12
2	0.3	600	150	23	210	20	12
3	0.5	600	210	20	210	20	12
4	0.7	600	210	20	150	23	12
5	0.9	600	210	20	100	20	12

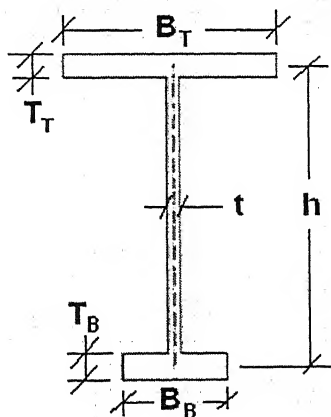


Fig 2.1 Beam Cross-section

The critical bending stresses f_{cb} for three types of load are calculated as per three codal specifications for the beam sections in Table 2.1. A wide range of L/r_y ratio (100-300) is taken. The results are shown graphically in Figures 2.2-2.4 for $\rho = 0.1, 0.5, 0.9$ only. Based on these plots, following observations are drawn:

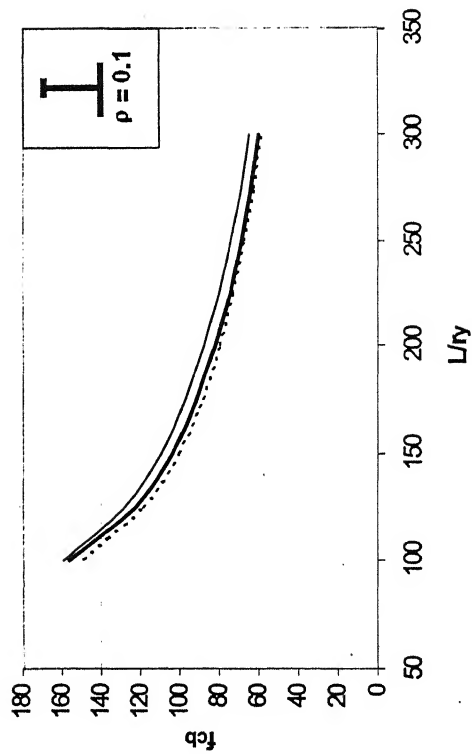
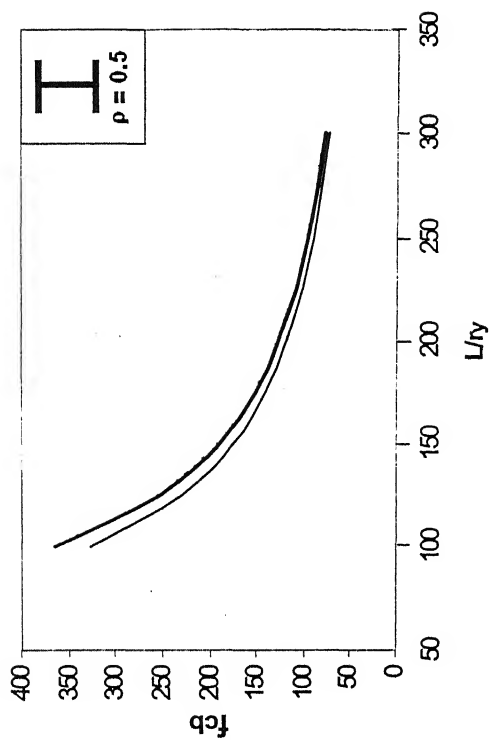
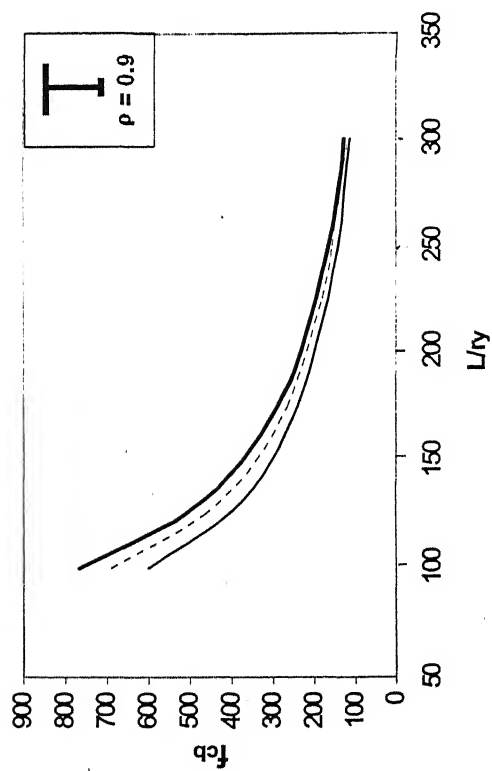
Uniform Moment: Values of f_{cb} as per three codal specifications are nearly the same for all cross-sections and L/r_y ratios.

Point Load (top flange): Values of f_{cb} are very close for the symmetric section ($\rho = 0.5$). While IS: 800 (1984) and SSRC specifications give close results, the new IS: 800 (draft) yields much higher (for $\rho = 0.9$) and lower (for $\rho = 0.1$) values of f_{cb} .

Point Load (bottom flange): There is no specific trend in results. For a symmetric section ($\rho = 0.5$), new IS: 800 (draft) gives results closer to SSRC guidelines while IS: 800 (1984) yields much lower values of f_{cb} . For, $\rho = 0.9$ and 0.1 results from IS: 800 specifications differ significantly from those of SSRC specifications.

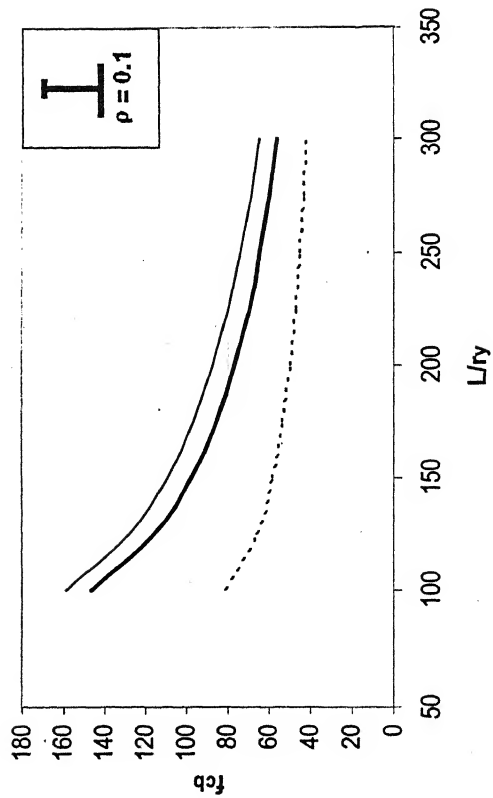
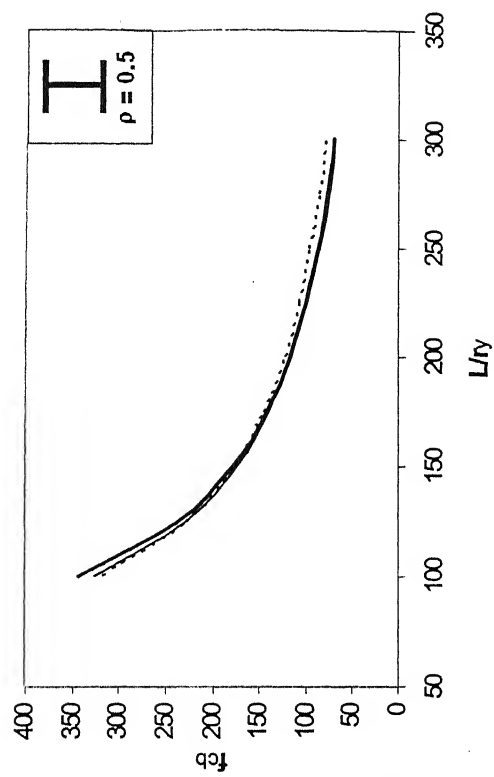
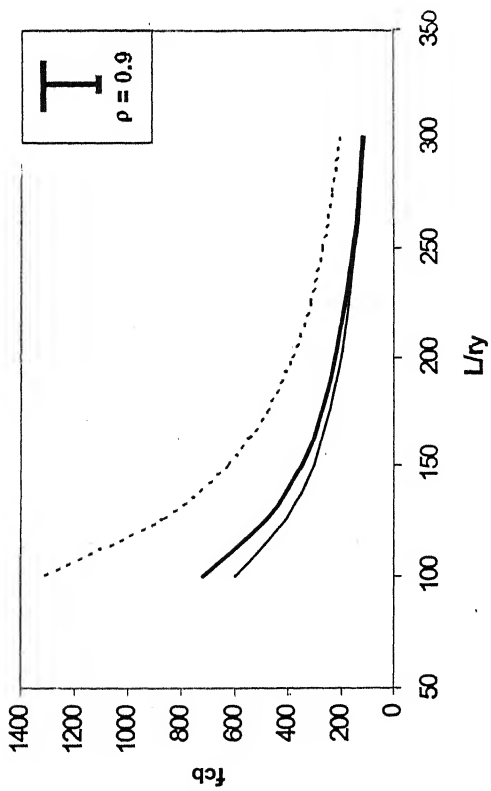
UDL (top flange): For, $\rho = 0.9$ and 0.5 , values of f_{cb} based on all three codal specifications are nearly the same. However, for $\rho = 0.1$, IS: 800 (1984) specification results in much higher value of f_{cb} for all L/r_y ratios.

UDL (bottom flange): Results based on new IS: 800 (draft) and SSRC specification are almost the same for all L/r_y ratios and all ρ values. IS: 800 (1984) also gives similar values of f_{cb} for $\rho \geq 0.5$ but yields higher values for $\rho < 0.5$.



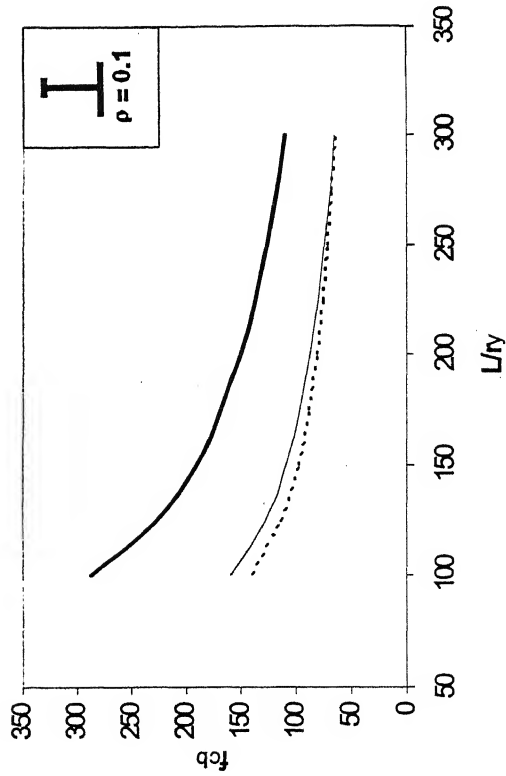
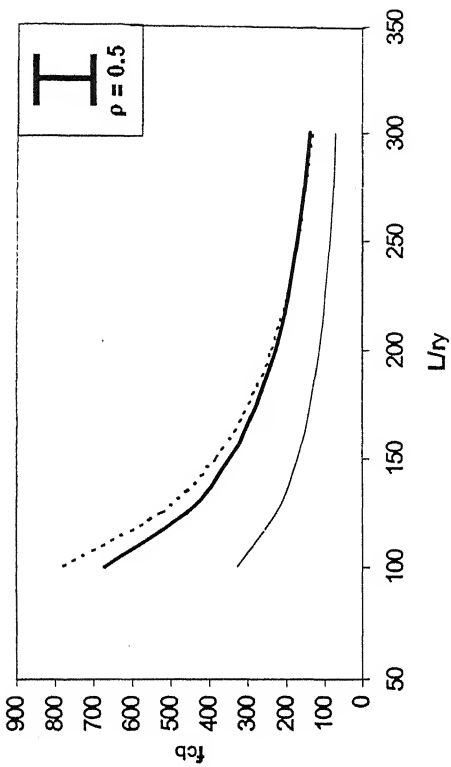
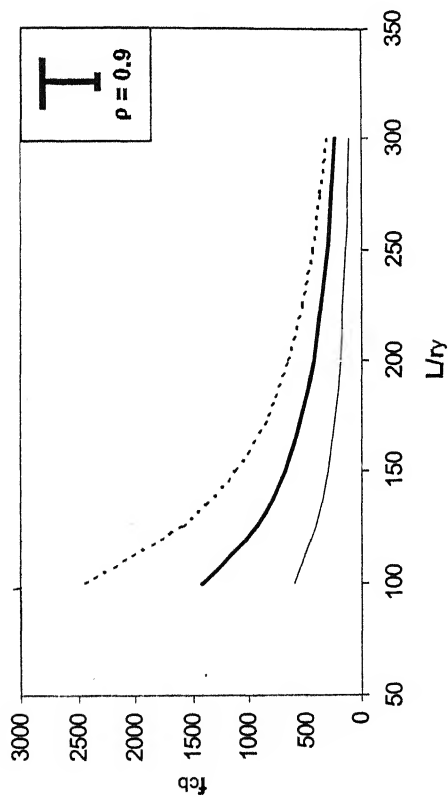
— IS: 800 (1984)
 - - - IS: 800 (Draft)
 — SSRC Guidelines

Fig 2.2 Comparison of Critical Bending Stress, f_{cb} (MPa):
 Uniform Moment ($\rho = 0.9, 0.5, 0.1$)



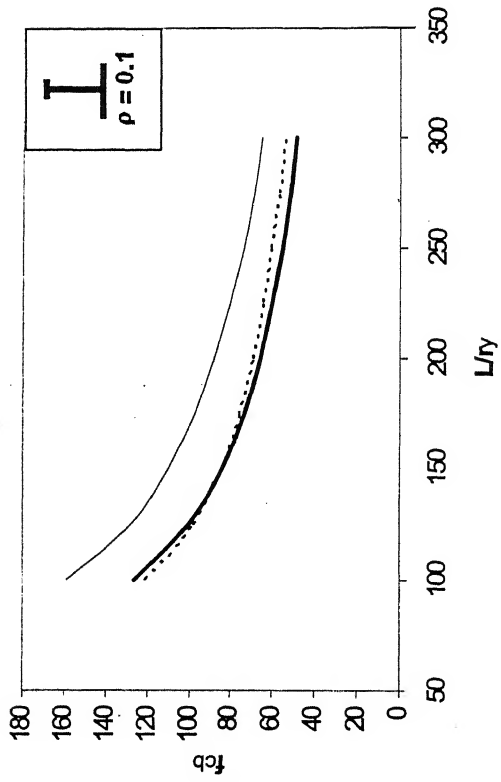
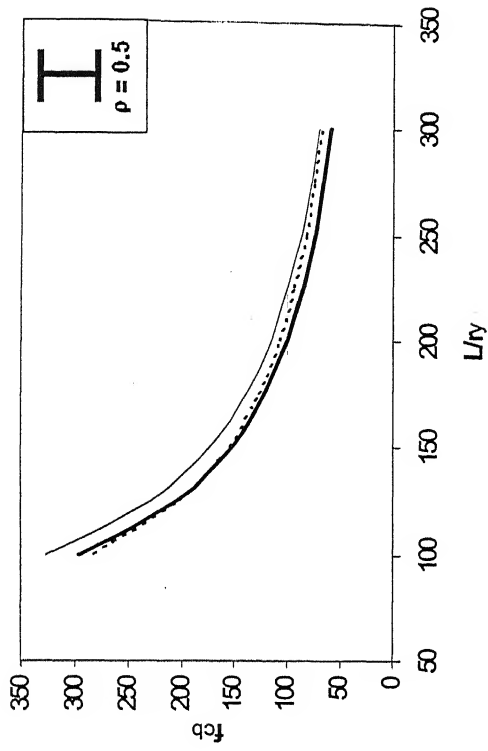
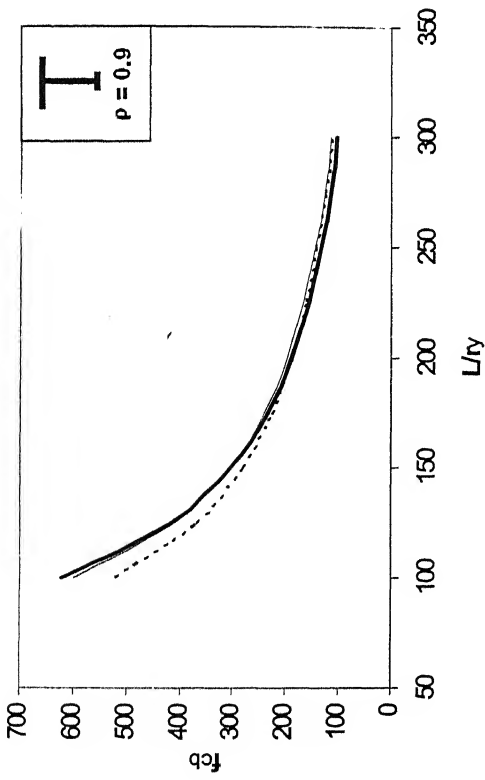
— IS: 800 (1984)
 - - - IS: 800 (Draft)
 — SSRC Guidelines

Fig 2.3a Comparison of Critical Bending Stress, f_{cb} (MPa) :
 Point Load at Top Flange ($\rho = 0.9, 0.5, 0.1$)



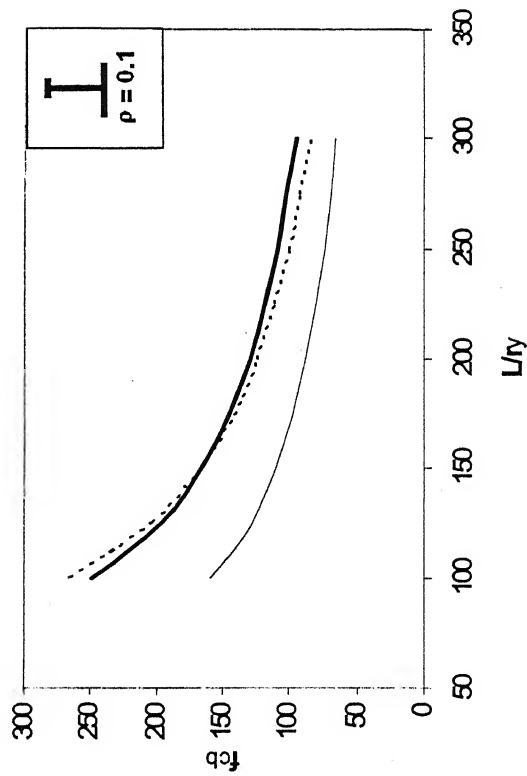
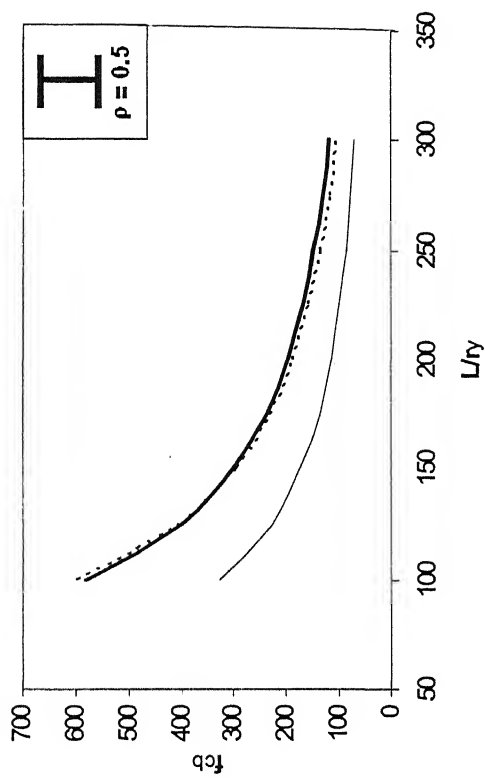
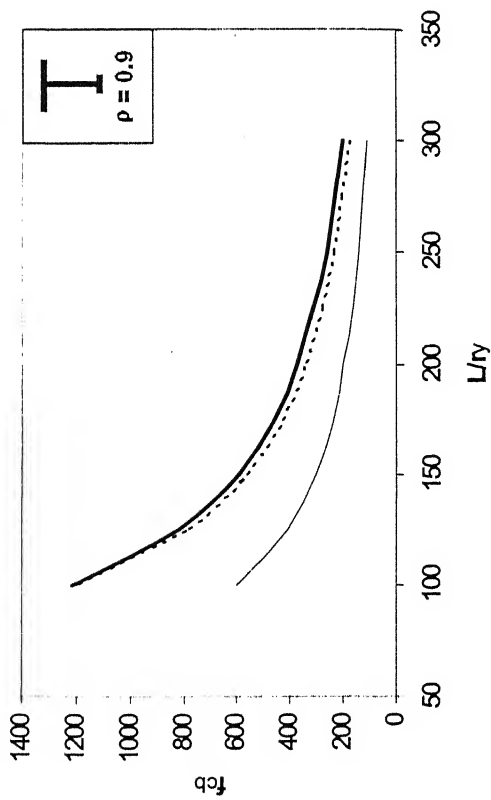
— IS: 800 (1984)
 - - - IS: 800 (Draft)
 — SSRC Guidelines

Fig 2.3b Comparison of Critical Bending Stress, f_b (MPa):
 Point Load at Bottom Flange ($\rho = 0.9, 0.5, 0.1$)



— IS: 800 (1984)
 - - - IS: 800 (Draft)
 — SSRC Guidelines

**Fig 2.4a Comparison of Critical Bending Stress, f_{cb} (MPa):
 UDL at Top Flange ($\rho = 0.9, 0.5, 0.1$)**



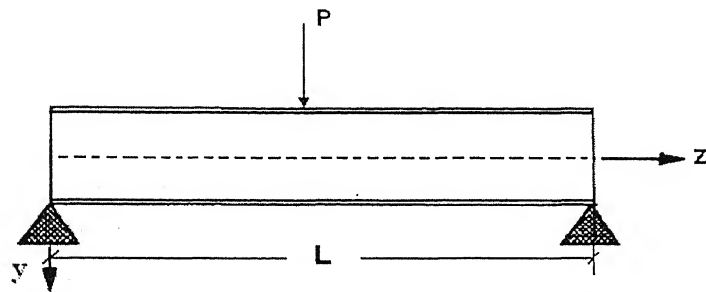
— IS: 800 (1984)
 - - - IS: 800 (Draft)
 — SSRC Guidelines

Fig 2.4b Comparison of Critical Bending Stress, f_{cb} (MPa):
 UDL at Bottom Flange ($\rho = 0.9, 0.5, 0.1$)

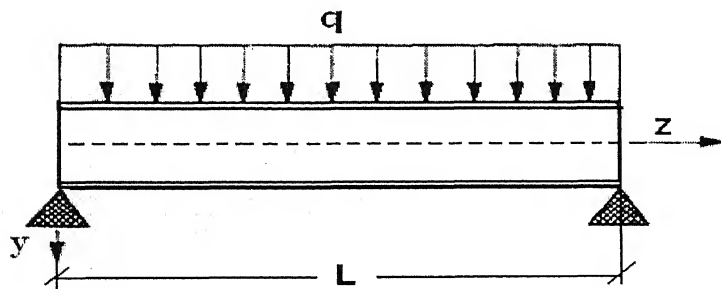
SIMPLY-SUPPORTED BEAMS

3.1 Introduction

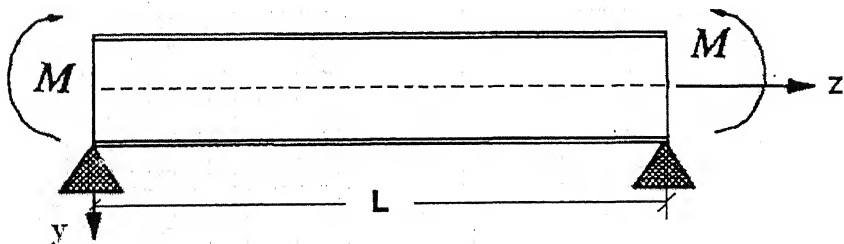
In this chapter, distortional buckling of simply-supported monosymmetric I-beams is studied for three types of load: a central point load, a uniformly distributed load and a uniform moment. These load cases are shown in Fig. 3.1.



Central Point Load



Uniformly Distributed Load



Uniform Moment

Fig. 3.1 Load Cases Considered

A typical monosymmetric I-section is shown in Fig 3.2. It is found convenient to define the properties of the I-section beam using the following parameters (Kitipornchai and Trahair, 1980):

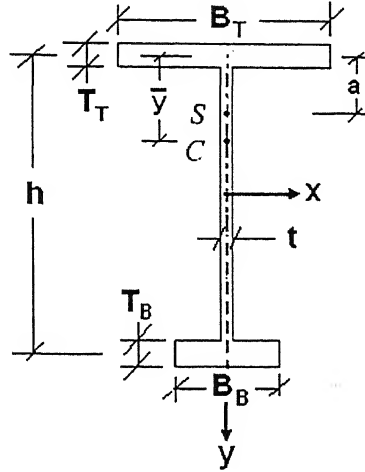


Fig 3.2 Beam Cross-section

$$(i) \quad I_Y = \int_A x^2 dA = I_{YT} + I_{YB} \quad (3.1)$$

$$I_{YT} = \frac{T_T B_T^3}{12}; \quad I_{YB} = \frac{T_B B_B^3}{12}$$

$$(ii) \quad J = \sum \frac{BT^3}{3} \quad (3.2)$$

in which B and T are the width and thickness of a typical rectangular element of the section.

(iii) The degree of beam mono-symmetry:

$$\rho = \frac{I_{YT}}{I_{YT} + I_{YB}} = \frac{I_{YT}}{I_Y} \quad (3.3)$$

in which I_{YT} , I_{YB} and I_Y are the second moment of area about the section y-axis of the top flange, bottom flange, and the whole section respectively. For an equal flange section $\rho = 0.5$, for a T-section $\rho = 1.0$ and for an inverted T-section $\rho = 0$.

(iv) Position of the shear centre from the top:

$$a = (1 - \rho)h \quad (3.4)$$

(v) Warping section constant:

$$I_w = \rho(1 - \rho)I_y h^2 \quad (3.5)$$

For a doubly symmetric I-section, $I_w = I_y h^2 / 4$ and for a T-section, $I_w = 0$.

(vi) Beam parameter:

In most of the studies, the following beam parameter has been used:

$$K = \sqrt{\frac{\pi^2 EI_w}{GJL^2}} \quad (3.6)$$

where GJ is the torsional rigidity, EI_w is the warping rigidity. This beam parameter K is zero for T-beams, which leads to computational difficulties in some situations. Hence, the choice of \bar{K} , a modified beam parameter, has been suggested by Kitipornchai and Trahair (1980):

$$\bar{K} = \sqrt{\frac{\pi^2 EI_y h^2}{4GJL^2}} \quad (3.7)$$

3.2 Moment Capacities under Flexural-torsional Buckling

3.2.1 Uniform Moment

Kitipornchai et al (1986) investigated the lateral-torsional buckling behaviour of monosymmetric I-beams under moment gradient and suggested the following expression for the non-dimensional elastic buckling moment, γ_c :

$$\gamma_c = \frac{M_c L}{\sqrt{EI_y GJ}} = m\pi \left[\sqrt{1 + 4\rho(1 - \rho)\bar{K}^2 f_1 + \left(\frac{\beta_x}{h} f_2 \bar{K}\right)^2} + \frac{\beta_x}{h} f_2 \bar{K} \right] \quad (3.8)$$

in which

$$\frac{1}{m} = 0.53 \sqrt{1 - 1.54\beta + \beta^2}$$

β_x is the monosymmetric property. For beams with $I_x/I_y < 0.5$, β_x is defined as:

$$\frac{\beta_x}{h} = 0.9(2\rho - 1) \left[1 - \left(\frac{I_y}{I_x} \right)^2 \right] \quad (3.9)$$

$$f_1 = 1 + 3\left(\frac{\beta_x}{h}\right)^2 \left(\frac{1+\beta}{2}\right)^\eta$$

$$f_2 = m\left(\frac{1-\beta}{2}\right) + \left(\frac{2\beta_x}{h}\right)\left(\frac{1+\beta}{2}\right)^\eta \quad \text{where} \quad \eta = \frac{9(1+\rho)}{1+\bar{K}}$$

β can take any value from -1 to +1. For uniform moment $\beta = -1$, $m = f_1 = f_2 = 1$ and

$$\gamma_c = \frac{M_c L}{\sqrt{EI_y GJ}} = \pi \left[\sqrt{1 + 4\rho(1-\rho)\bar{K}^2 + \left(\frac{\beta_x}{h}\bar{K}\right)^2 + \frac{\beta_x}{h}\bar{K}} \right]$$

3.2.2 Central Point Load

Wang and Kitipornchai (1986) investigated the lateral-torsional buckling behaviour of monosymmetric I-beams under a central point load and suggested the following expression for the non-dimensional elastic buckling moment, γ_c :

$$\gamma_c = \frac{PL^2}{4\sqrt{EI_y GJ}} = \bar{m} \pi \left[\sqrt{1 + 4\rho(1-\rho)\bar{K}^2 + (f_1 \bar{K})^2 \left(\zeta + \frac{\beta_x}{h} f_2\right)^2 + f_1 \bar{K} \left(\zeta + \frac{\beta_x}{h} f_2\right)} \right] \quad (3.10)$$

in which
$$\bar{m} = \frac{\left(\frac{\pi^2}{2}\right)}{\sqrt{1 + \left(1 + \frac{\pi^2}{4}\right)^2}}; \quad f_1 = \frac{4\bar{m}}{\pi^2}; \quad f_2 = \frac{1}{2}\left(\frac{\pi^2}{4} - 1\right)$$

and

$$\zeta = \begin{cases} = -2(1-\rho) & \text{for top flange loading} \\ = 0 & \text{for shear center loading} \\ = 2\rho & \text{for bottom flange loading} \end{cases}$$

3.2.3 Uniformly Distributed Load

For this case, Wang and Kitipornchai (1986) suggested the following expression for the non-dimensional elastic buckling moment, γ_c :

$$\gamma_c = \frac{qL^3}{8\sqrt{EI_y GJ}} = \bar{m} \pi \left[\sqrt{1 + 4\rho(1-\rho)\bar{K}^2 + (f_1 \bar{K})^2 \left(\zeta + \frac{\beta_x}{h} f_2\right)^2 + f_1 \bar{K} \left(\zeta + \frac{\beta_x}{h} f_2\right)} \right]$$

in which

$$\bar{m} = \frac{(\frac{\pi^2}{2})}{\sqrt{(\frac{3}{4})^2 + (1 + \frac{\pi^2}{3})^2}}; \quad f_1 = \frac{4\bar{m}}{\pi^2}; \quad f_2 = \frac{1}{2}(\frac{\pi^2}{3} - 1)$$

and

$$\zeta = \begin{cases} = -2(1-\rho) & \text{for top flange loading} \\ = 0 & \text{for shear center loading} \\ = 2\rho & \text{for bottom flange loading} \end{cases}$$

The above expressions for the moment capacity of beams under different load cases are used to calculate the buckling capacity of beams under flexural-torsional buckling; these values are used for comparison of results to highlight the effect of considering the distortional buckling behaviour of beams.

3.3 Present Investigation

The main aim of this chapter is to study the distortional buckling of simply-supported I-beams for three types of load shown in Fig. 3.1 for different degrees of monosymmetry of beams. Top-flange and bottom-flange load positions are considered for the first two load cases. ABAQUS (2004) is used in the present investigation to obtain the results. In order to show the effect of distortional buckling, results are compared with existing solutions which consider lateral-torsional buckling only. The moment modification factors for different load cases are calculated with respect to the case of a uniform moment considering only flexural-torsional buckling. These moment modification factors are also compared with the provisions in SSRC Guidelines (1998).

The beam sections given in Table 2.1 of chapter 2 are used for the finite element modeling using ABAQUS. The size of the flanges is changed to vary the degree of monosymmetry; size of one flange is fixed at 210mm X 20mm while the size of the other flange is varied. The web thickness and the distance between the flange centroids are kept as 12mm and 600mm, respectively. The monosymmetry parameter ρ varies from 0.1 to 0.9. The span-to-depth ratios (L/h) from 2 to 8 are considered here.

For the finite element modeling, the flanges and webs are modeled with S8R5 elements (*eight-node shell element with five degrees of freedom per node*). Eigen value analyses are conducted to determine buckling loads. The Young's modulus E is taken as 206.6 GPa and the Poisson's ratio ν as 0.3. Quadratic shell elements (S8R5) with five degrees of freedom (three displacement components and two in-surface rotation components) are chosen because they give accurate results for thin shells in large rotations, small-strain simulations. The change in thickness with deformation is ignored in these elements; it would be required to be considered only in a geometrically nonlinear analysis.

3.4 Buckling Loads

In figures that follow (Figs.3.3 to 3.5) the results are presented in terms of non-dimensional quantities. The load is non-dimensionalized as

$$\begin{aligned}
 P \frac{L^2}{4\sqrt{EI_y GJ}} & \quad (\text{point load}) \\
 q \frac{L^3}{8\sqrt{EI_y GJ}} & \quad (\text{uniformly distributed load}) \\
 M \frac{L}{\sqrt{EI_y GJ}} & \quad (\text{uniform moment})
 \end{aligned} \tag{3.12}$$

and \bar{K} , as given by Eq. 3.7, is the non-dimensional beam parameter. For beam-sections considered in this investigation (Table 2.1), the range of \bar{K} from 1 to 6 corresponds to beam-length of 4.8m to 1.2m.

Results for a mid-span point load are shown in Fig. 3.3a, b, for a uniformly distributed load in Fig. 3.4a, b and for a uniform moment in Fig. 3.5. In all figures, firm lines are the results for distortional buckling and dashed lines represent results for flexural-torsional buckling as obtained from expressions given in sec. 3.2. In all cases, the results match with those of Ma and Hughes (1996) for a symmetric I-section, i.e. for $\rho=0.5$.

Trends in results are similar for a point load (Fig. 3.3) and a uniformly distributed load (Fig. 3.4). For long beams (in the present case, $0 < \bar{K} < 1.2$) critical loads for flexural-

torsional buckling and distortional buckling are almost same. However, in case of short beams ($\bar{K} > 1.2$), distortional buckling is predominant. So, analysis of such beams without taking distortion of web into consideration may give highly overestimated critical loads. It is also seen that critical loads are higher when the load is at the bottom flange than that at the top flange. On the other hand, for the case of uniform moment (Fig. 3.5), it is observed that the critical loads remain, more or less, the same for lateral-torsional buckling as well as for distortional buckling. This holds good for all types of sections and for all spans considered.

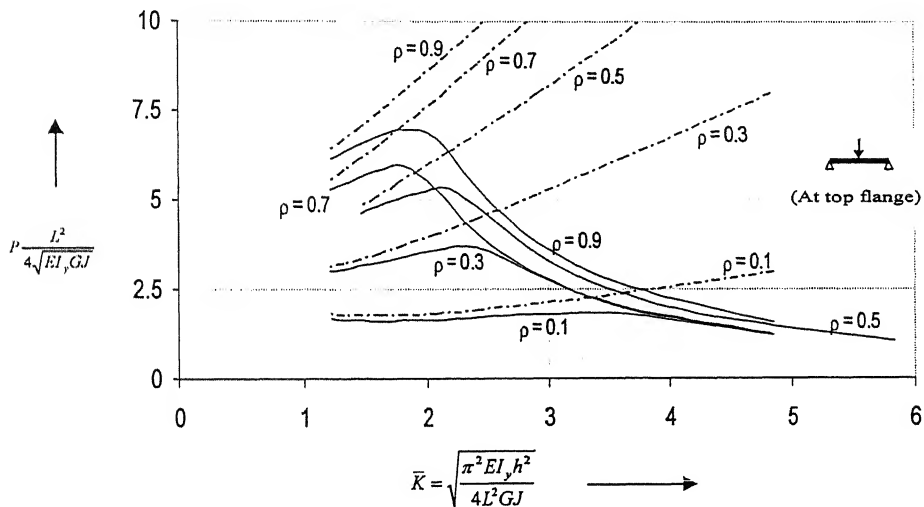


Fig. 3.3a Variation in Buckling Loads: Point Load at Top Flange
[distortional (—) and torsional (-----)]

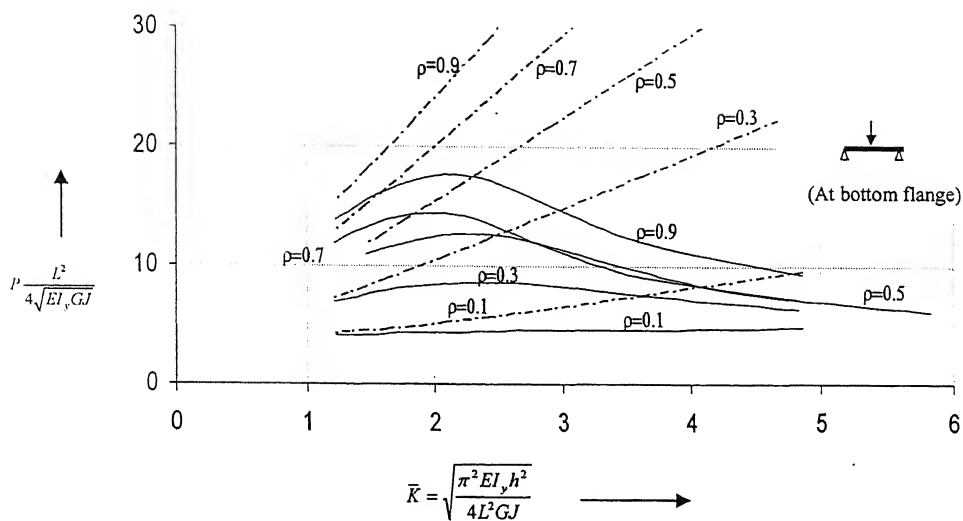


Fig. 3.3b Variation in Buckling Loads: Point Load at Bottom Flange [distortional (—) and torsional (-----)]

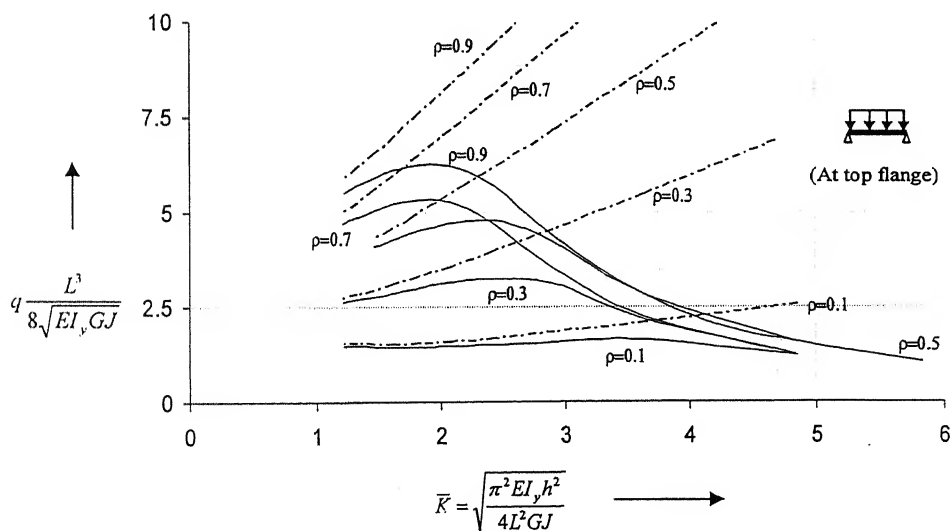


Fig. 3.4a Variation in Buckling Loads: UDL at Top Flange [distortional (—) and torsional (-----)]

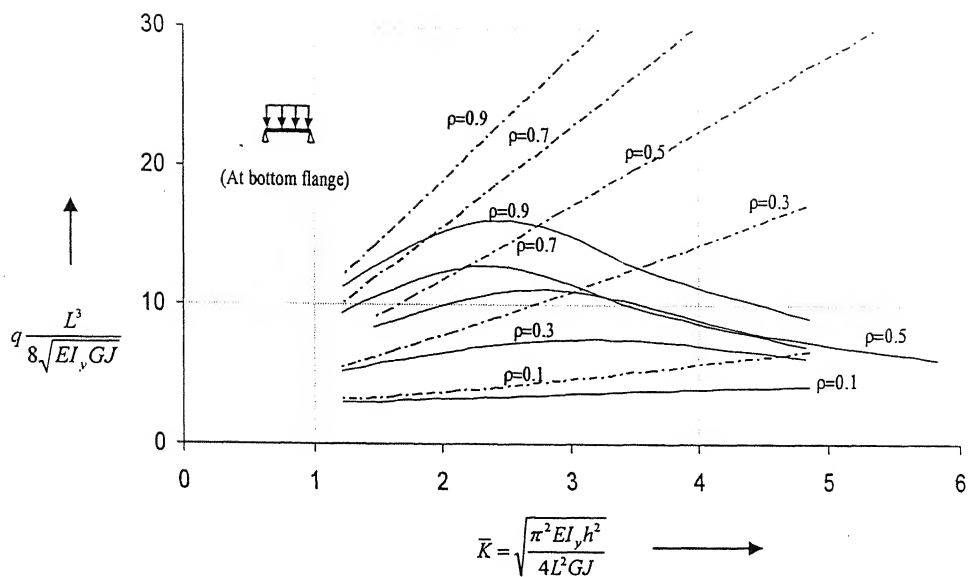


Fig. 3.4b Variation in Buckling Loads: *UDL at Bottom Flange*
[distortional (—) and torsional (-----)]

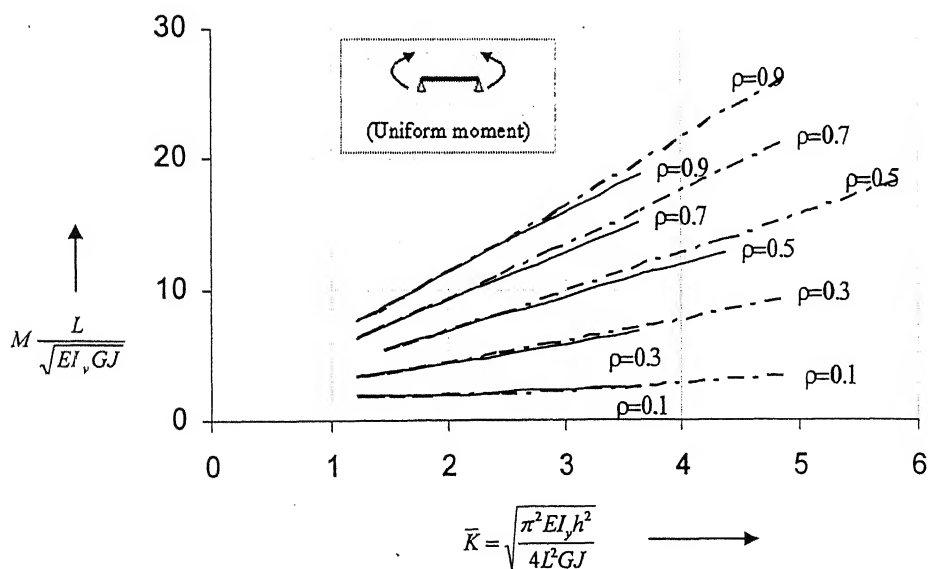
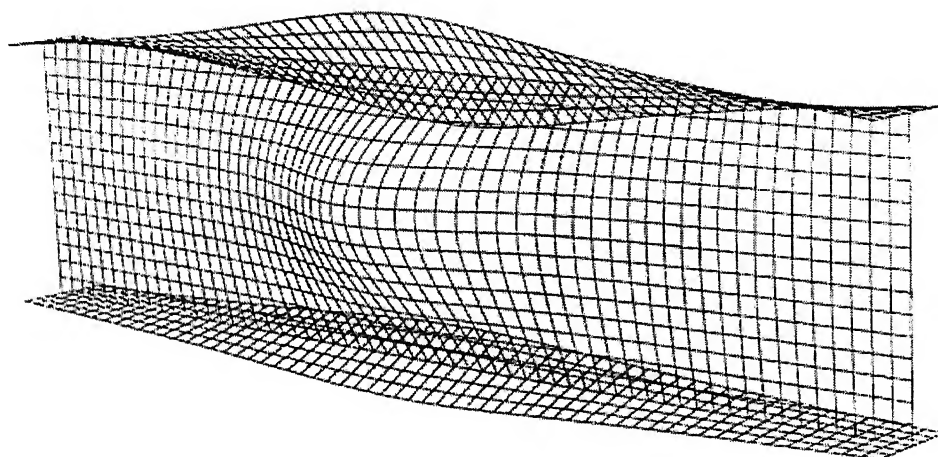
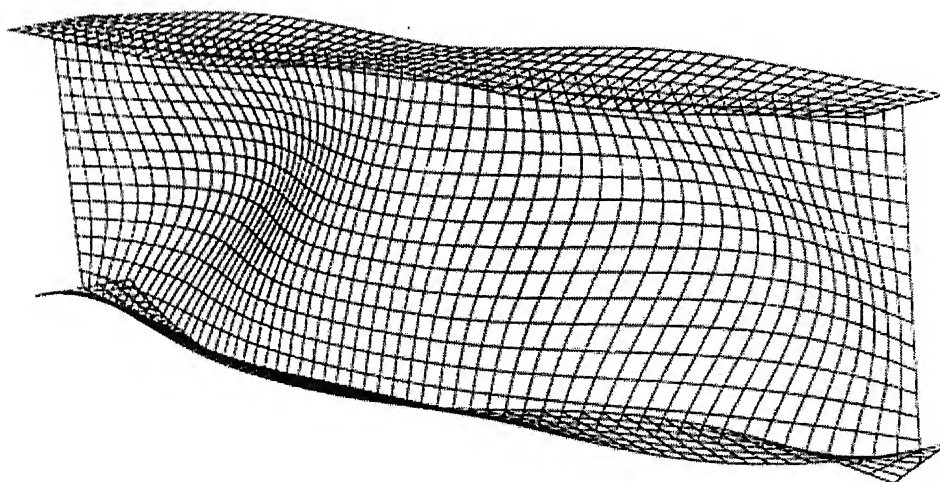


Fig. 3.5 Variation in Buckling Loads: *Uniform Moment*
[distortional (—) and torsional (-----)]

The buckled beam shapes under top & bottom flange point loads are shown in Fig. 3.6 for $L/h = 4$ and in Fig. 3.7 $L/h = 8$. These are for a doubly symmetric section, $\rho = 0.5$. As can be seen in these figures, the effect of distortional buckling is much more in a short beam ($L/h = 4$) but for a longer beam ($L/h = 8$) the effect of distortional buckling is very little; practically the beam has buckled in a lateral-torsional mode.

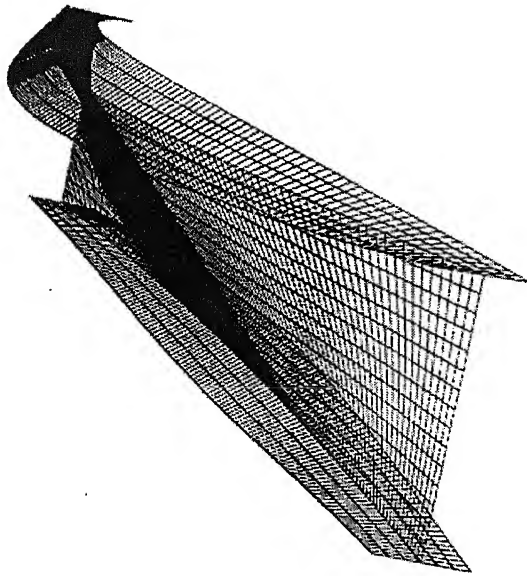


Load at Top Flange

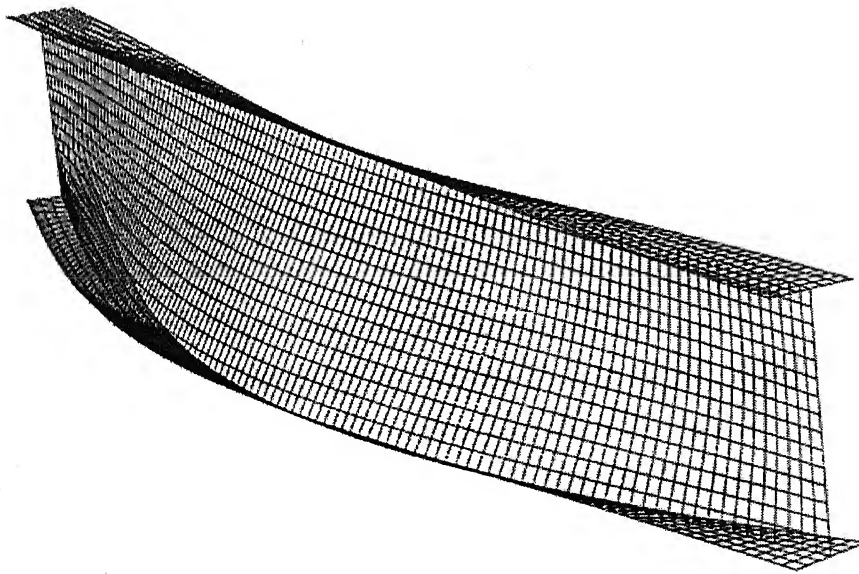


Load at Bottom Flange

**Fig. 3.6 Buckled Shape in Simply Supported Beam ($L/h = 4$):
Point Load at Mid Span**



Load at Top Flange



Load at Bottom Flange

**Fig. 3.7 Buckled Shape in Simply Supported Beam ($L/h = 8$):
Point Load at Mid Span**

3.5 Moment Modification Factors

As stated in Chapter 2, many design specifications provide solutions for flexural-torsional buckling with uniform moment loading. To take into account different load cases, a factor called Moment Modification Factors, C_b , is applied to the solutions with uniform moment only.

SSRC Guideline (1998) has recommended the expression (Eq. 2.9) for C_b for beams under single curvature bending; this expression is reproduced below for convenient reference.

$$C_b = \frac{12.5M_{\max}}{2.5M_{\max} + 3M_A + 4M_B + 3M_C} (1.4^{2\xi/h}) \quad (3.13)$$

For results of this investigation, the C_b factor is calculated by dividing the maximum moment at buckling by the moment capacity of the beam subjected to a uniform moment; that is:

$$C_{b(ABAQUS)} = \frac{M_{cr(\text{moment gradient})}}{M_{cr(\text{uniform moment})}} \quad (3.14)$$

The value of the $M_{cr(\text{moment gradient})}$ in (Eq. 3.14) is the maximum moment within the unbraced length; e.g. for a simply supported beam with length L with no intermediate bracing between supports and a point load at mid-span, $M_{cr(\text{moment gradient})} = P_{cr} L/4$, where P_{cr} is the resulting critical load. Here, $M_{cr(\text{uniform moment})}$ is the moment at buckling in the flexural-torsional mode, while $M_{cr(\text{moment gradient})}$ is for distortional buckling of the beam.

In the following figures (Figs. 3.8 & 3.9), moment modification factors $C_{b(ABAQUS)}$ is compared with the C_b based on SSRC Guidelines. Firm lines are for ABAQUS results and dashed lines correspond to solution based on SSRC Guidelines. As can be seen in these figures, the effect of distortional buckling is evidently more pronounced in short beams and when the compression (top) flange is bigger than the tension (bottom) flange ($\rho > 0.5$).

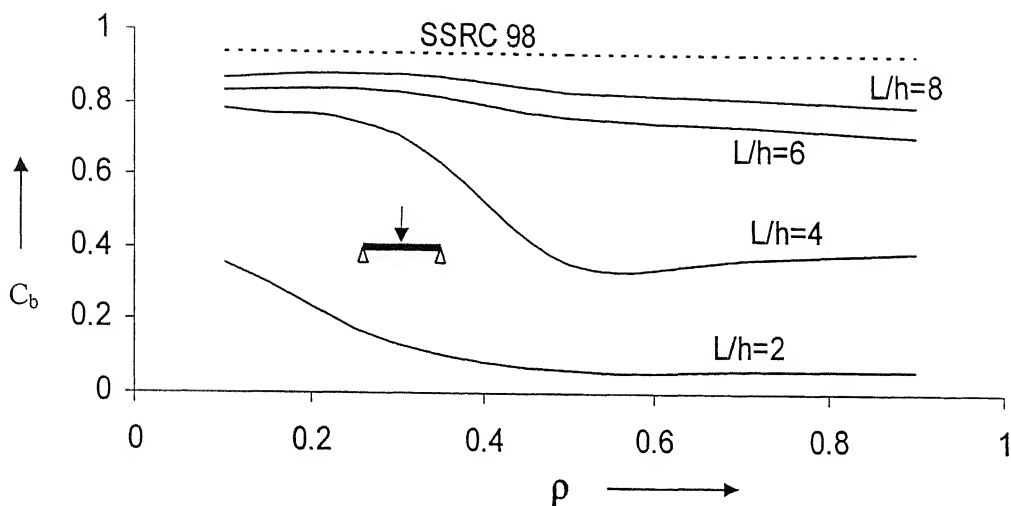


Fig. 3.8a Comparison of Moment Modification Factors C_b with ρ :
Point Load at Top Flange [$\rho=0$: \perp , $\rho=0.5$: I, $\rho=1$: T]

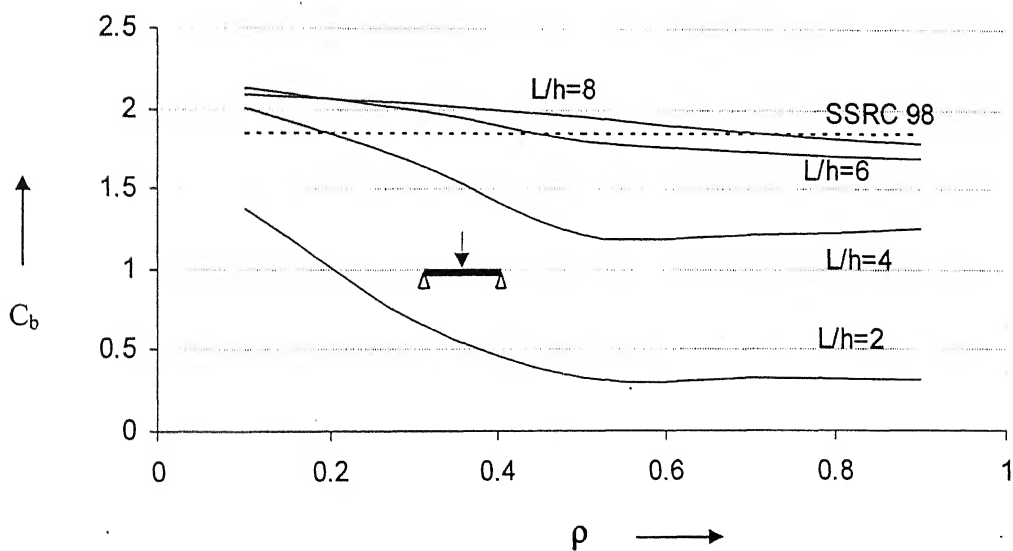


Fig. 3.8b Comparison of Moment Modification Factors C_b with ρ :
Point Load at Bottom Flange [$\rho=0$: \perp , $\rho=0.5$: I, $\rho=1$: T]

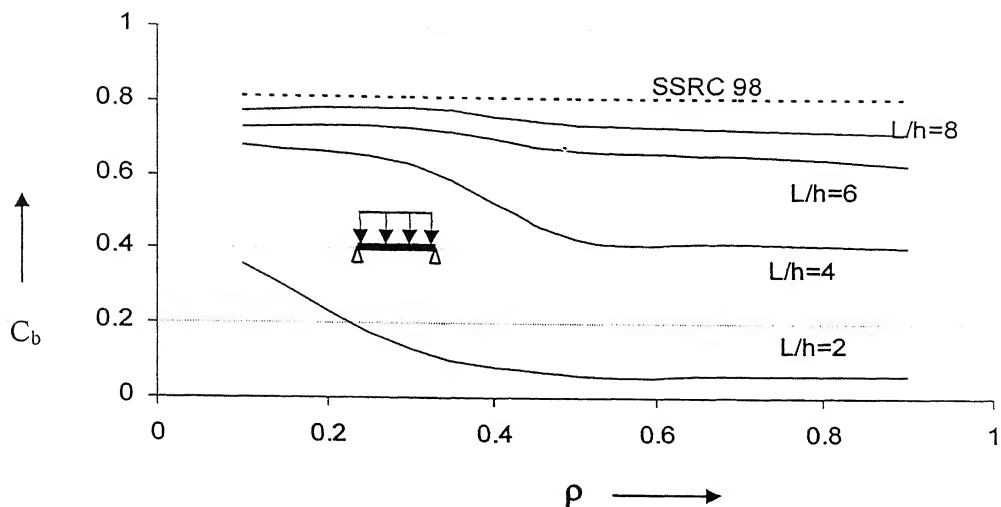


Fig. 3.9a Comparison of moment modification factors C_b with ρ :
UDL at Top Flange [$\rho = 0$: \perp , $\rho = 0.5$: I, $\rho = 1$: T]

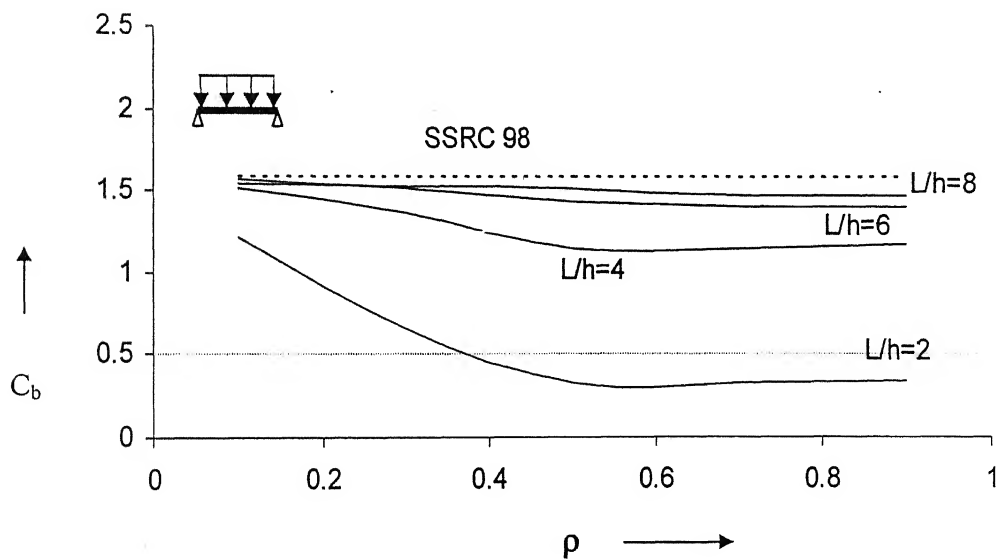


Fig. 3.9b Comparison of moment modification factors C_b with ρ :
UDL at Bottom Flange [$\rho = 0$: \perp , $\rho = 0.5$: I, $\rho = 1$: T]

3.6 Concluding remarks

While investigating lateral buckling problems most of the researchers assume that the beam cross-section remains undistorted. This approach gives reasonable results for long beams because the buckling phenomenon is guided by the flexural-torsional buckling mode. But, in case of short beams distortional buckling is predominant and so flexural-torsional buckling solutions may give overestimated critical loads.

SSRC Guidelines (1998) recommendations for moment modification factors are nearly the same as those obtained in this investigation for fairly long beams only. For short beams the difference is significant since C_b values are dependent on the degree of beam mono-symmetry ρ , as well as on the L/h ratio. So, care must be taken while designing such short beams.

PROPPED-CANTILEVER BEAM: REVERSE-CURVATURE BENDING

4.1 Introduction

When beams having monosymmetric sections are subjected to reverse-curvature bending, the buckling phenomenon becomes more complex than the case with single curvature bending. Because of the reverse-curvature bending, both the top and bottom flanges are subjected to compression at different locations along the beam. Since the flanges are of different size in a monosymmetric section, the buckling strength of the beam may be governed by either the maximum moment causing compression in the top flange or the maximum moment causing compression in the bottom flange.

As mentioned in chapter 3, the concept of a Moment Modification Factor, C_b , is quite common in providing solutions for buckling in beams to account for different load cases; this factor is applied to the solutions with uniform moment loading. The SSRC Guidelines (1998) recommend the use of expression given by Eq. (2.10) for beams under reverse-curvature bending; this is reproduced below:

$$C_b = \frac{12.5M_{\max}}{2.5M_{\max} + 3M_A + 4M_B + 3M_C} (1.4^{2\xi/h})(0.5 + 2\rho^2) \quad 0.1 \leq \rho \leq 0.9 \quad (4.1)$$

The term $(0.5 + 2\rho^2)$ in the above equation is, in fact, a modifier to account for reverse-curvature bending on monosymmetric shapes; this modifier equals 1.0 for single-curvature bending as well as for a doubly symmetric section, $\rho = 0.5$. The factor $(1.4^{2\xi/h})$ in Eq. (4.1) accounts for the effect of load height.

Helwig et al. (1997) suggested a modification in the expression for C_b given by Eq. (4.1). Based on a rigorous finite element analysis, they proposed the upper limit of the value of C_b as 3.0. Accordingly, the expression of C_b with $0.1 \leq \rho \leq 0.9$, under reverse-curvature bending is:

$$C_b = \frac{12.5M_{\max}}{2.5M_{\max} + 3M_A + 4M_B + 3M_C} (0.5 + 2\rho^2) \leq 3.0 \quad (4.2)$$

For taking the effects of load heights, the value of C_b in Eq. (4.2) is to be multiplied by a factor to get the modified value C_b^* :

$$C_b^* = (1.4^{2\xi/h})C_b \quad (4.3)$$

4.2 Present Investigation

A propped cantilever beam is analyzed in the present investigation; this is one of the simpler cases of reverse-curvature bending in a single span beam. Two types of loads, a central point load and a uniformly distributed load (Fig. 4.1) are considered for different degrees of beam mono-symmetry. Both the top and the bottom-flange load positions are taken for these two load cases. ABAQUS is used in the present investigation. The case of a uniform sagging moment is also investigated to get the lateral-torsional buckling capacity of the propped-cantilever beam.

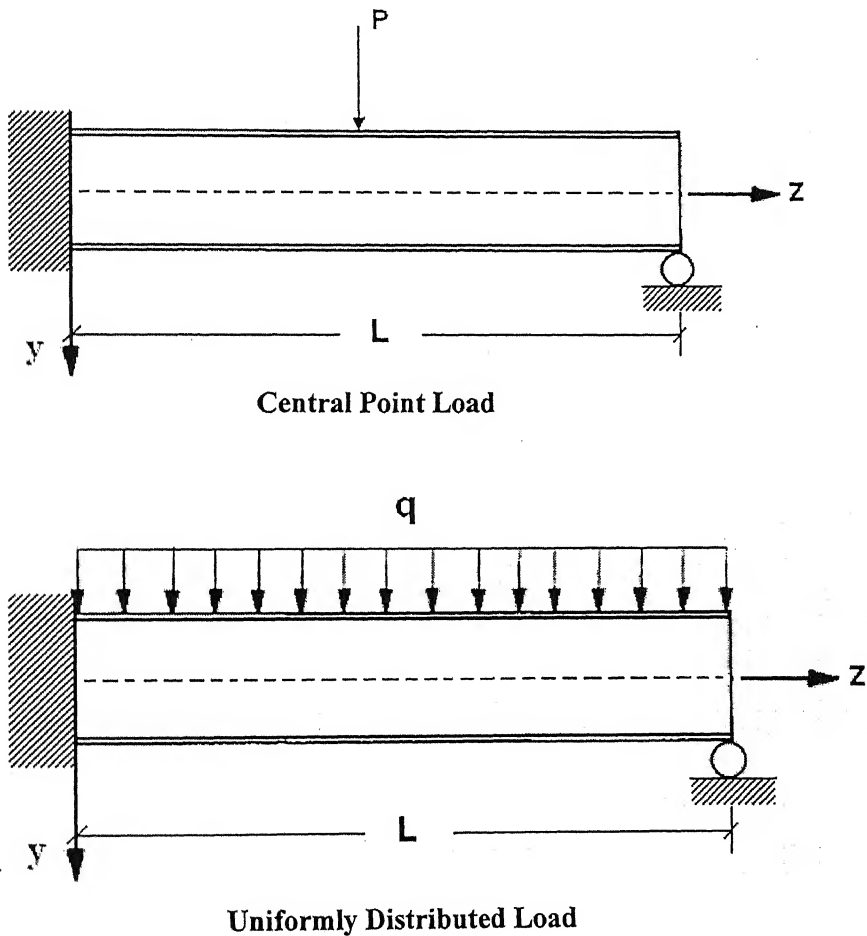


Fig. 4.1 Load Cases Considered

The following beam sections (Table 4.1) are used for the finite element modeling using ABAQUS:

Table 4.1 Beam Sections:

Section no.	ρ	h (mm)	B_T (mm)	T_T (mm)	B_B (mm)	T_B (mm)	t (mm)
1	0	600	0	0	210	20	12
2	0.1	600	100	20	210	20	12
3	0.3	600	150	23	210	20	12
4	0.5	600	210	20	210	20	12
5	0.7	600	210	20	150	23	12
6	0.9	600	210	20	100	20	12
7	1	600	210	20	0	0	12

The size of the flanges is changed to vary ρ , the degree of mono-symmetry of the cross-section. One of the flanges is fixed at 210mm X 20mm while the size of the other flange is varied. The web thickness is kept 12mm. The ratio ρ varies from 0 to 1.0. Span-to-depth ratios are kept in the range 4 to 12.

For the finite element modeling, the flanges and webs are modeled with S8R5 elements (*eight-node shell element with five degrees of freedom per node: three displacement components and two in-surface rotation components*). Eigen value analyses are conducted to determine buckling loads. The value of Young's modulus is taken as 206.6 GPa and that of Poisson's ratio as 0.3. For comparing the results of distortional buckling with those of lateral-torsional buckling, the latter are also obtained since these are not readily available in a form to facilitate the comparison. For modeling the beam sections for lateral-torsional buckling, same elements and the process as above is used. Closely spaced transverse stiffeners are used to avoid cross-sectional distortion. Shell elements are used to model transverse stiffeners, which are spaced at approximately half the girder depth.

4.3 Results

In figures that follow (Figs 4.2 & 4.3) the results are presented in terms of non-dimensional quantities. The load is non-dimensionalized as

$$P \frac{L^2}{4\sqrt{EI_y GJ}} \quad (\text{point load})$$

$$q \frac{L^3}{8\sqrt{EI_y GJ}} \quad (\text{uniformly distributed load}) \quad (4.4)$$

and the non-dimensional beam parameter \bar{K} is taken as given by Eq. (3.7). For beam-sections considered in this investigation (Table 4.1), the range of \bar{K} is from 0.8 to 3 which corresponds to a beam-length of 7.2m to 2.4m.

Results for a mid-span point load are given in Figs. 4.2a & 4.2b and for a uniformly distributed load in Figs. 4.3a & 4.3b. In all figures, results are for distortional buckling of beams. By and large, trends in results are similar for the two load cases. For $\rho \geq 0.3$ there is a peak in the distortional buckling load when the beam parameter \bar{K} is in the range 1.3 – 1.5 (which corresponds to beam-length of 5.4m to 3.85m).

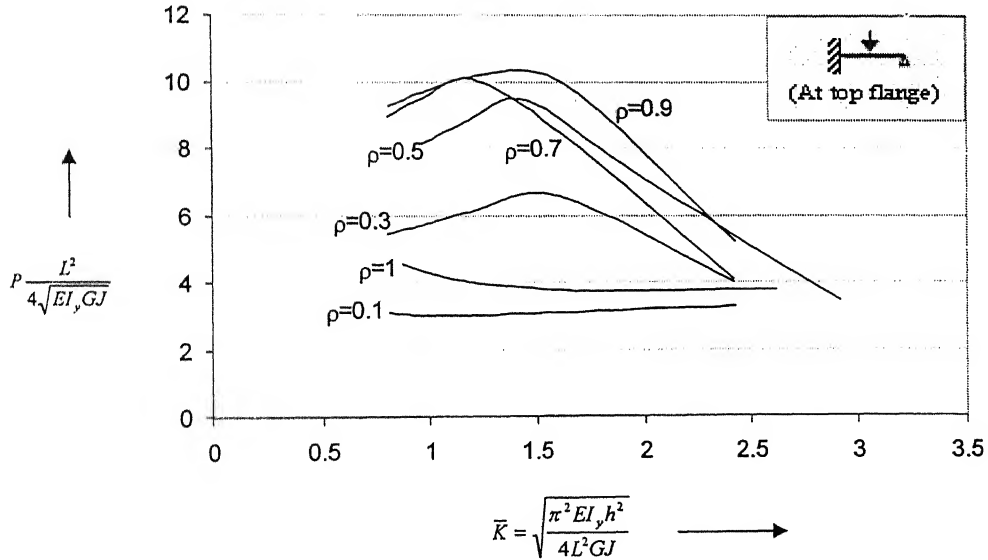


Fig. 4.2a Variation in Distortional Buckling Loads: Point Load at Top Flange

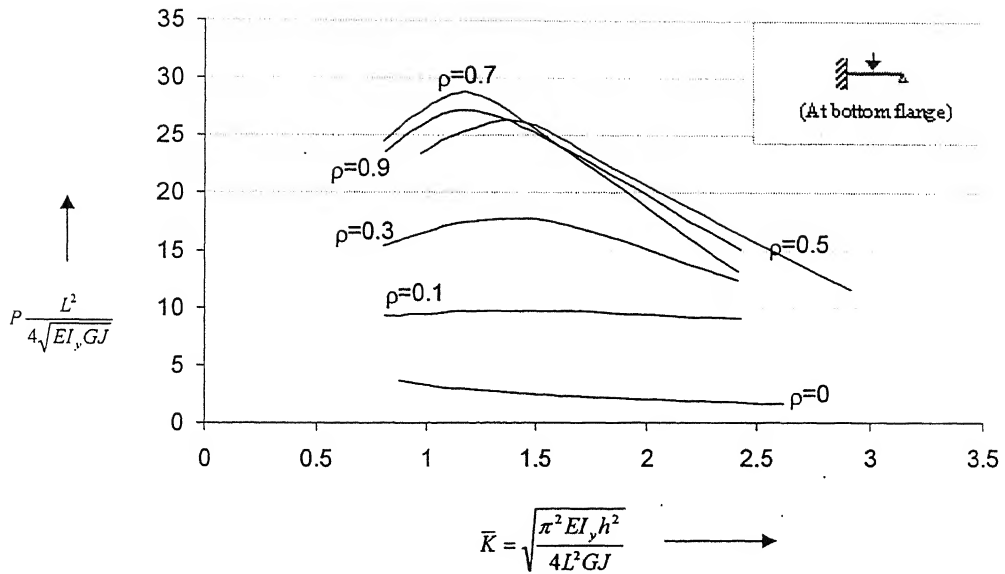


Fig. 4.2b Variation in Distortional Buckling Loads: *Point Load at Bottom Flange*

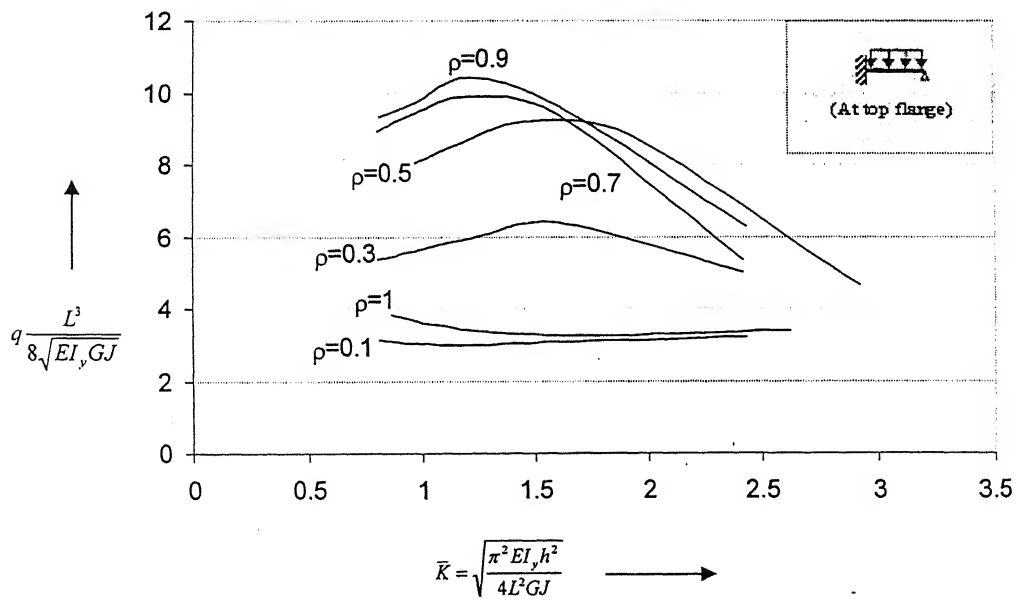


Fig. 4.3a Variation in Distortional Buckling Loads: *UDL at Top Flange*

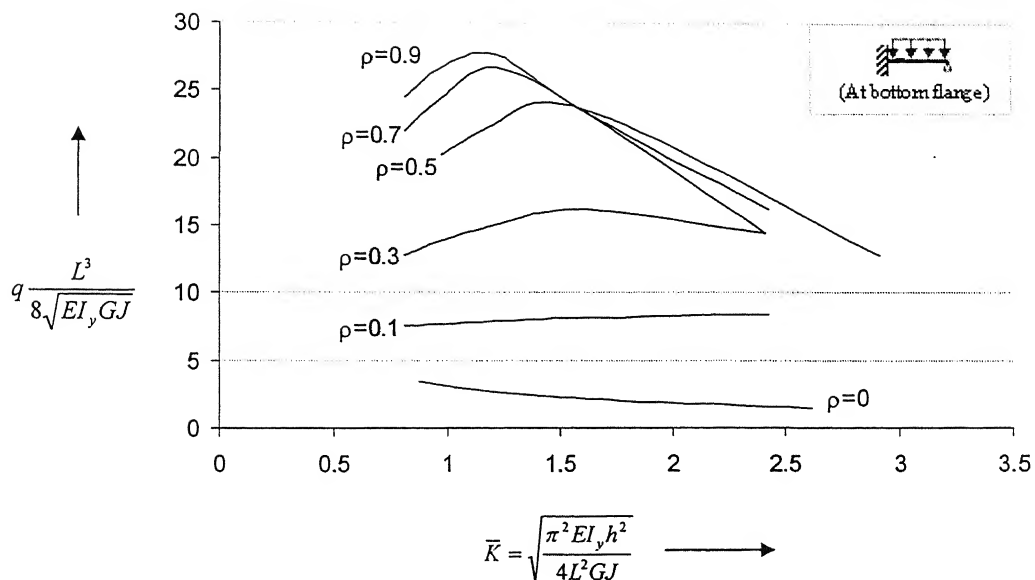
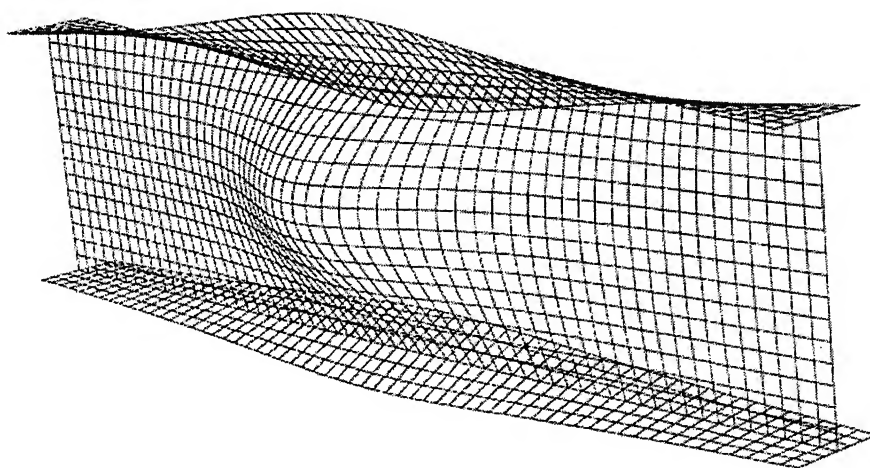
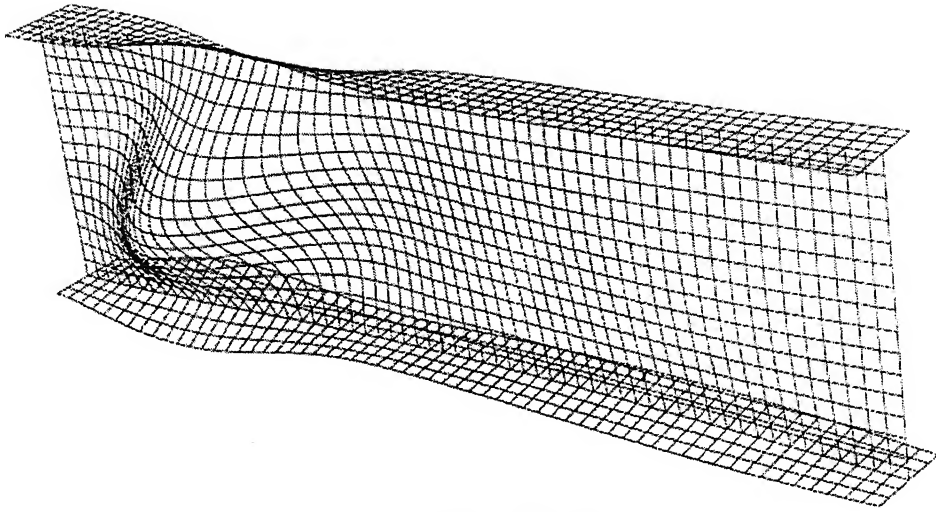


Fig. 4.3b Variation in Distortional Buckling Loads: UDL at Bottom Flange

In the following figures buckled beam shapes under top- & bottom-flange point loads are shown for a doubly symmetric beam section ($\rho = 0.5$) with $L/h = 4$ (Fig. 4.4) & $L/h = 10$ (Fig. 4.5). As can be seen, the effect of distortional buckling is much more in the short beam ($L/h = 4$) but for the longer beam ($L/h = 10$) the effect of distortional buckling is very less; practically the beam buckles in a lateral-torsional mode.

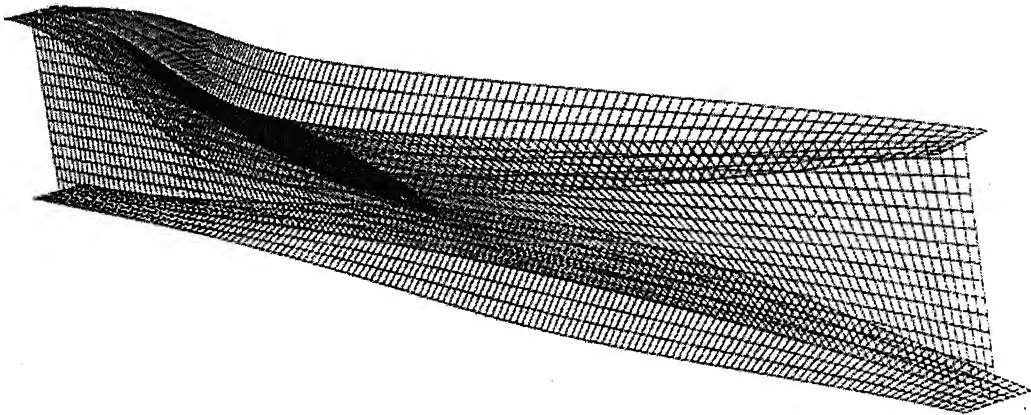


Load at Top Flange

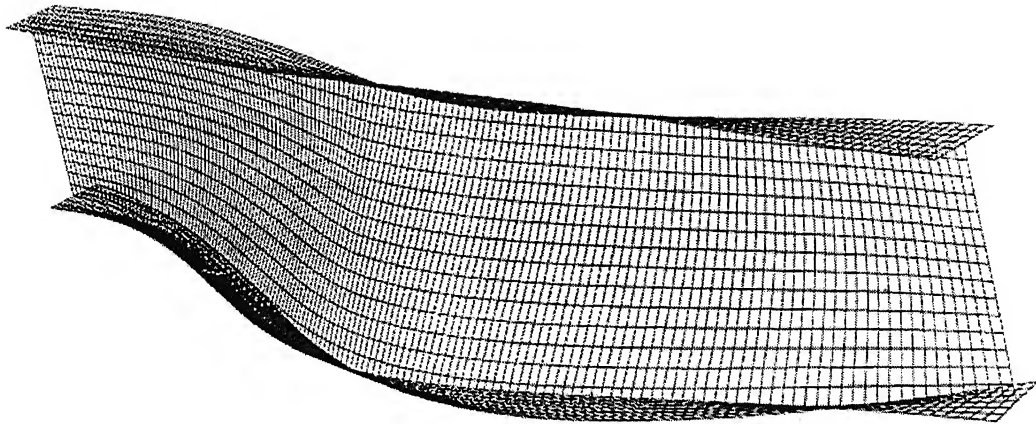


Load at Bottom Flange

**Fig. 4.4 Buckled Shape of a Propped-Cantilever Beam ($L/h=4$):
Point Load at Mid Span**



Load at Top Flange



Load at Bottom Flange

**Fig. 4.5 Buckled Shape of a Propped Cantilever Beam ($L/h=10$):
Point Load at Mid Span**

4.4 Moment Modification Factors

In this section a comparison is made of the moment modification factors which are obtained based on distortional buckling of beams, with those based on SSRC Guidelines (1998) and Helwig et al. (1997). For load cases considered in this investigation, the following quantity in Eqs. (4.1) and (4.2) is evaluated:

$$\frac{12.5M_{\max}}{2.5M_{\max} + 3M_A + 4M_B + 3M_C} = C \quad (\text{say})$$

(a) *Central point load*

$$M_{\max} = -6PL/32, \quad M_A = -PL/64, \quad M_C = 5PL/64, \quad M_B = 5PL/32$$

$$C = 1.70455$$

(b) *Uniformly distributed load*

$$M_{\max} = -16qL^2/128, \quad M_A = 0, \quad M_C = qL^2/16, \quad M_B = qL^2/16$$

$$C = 2.0833$$

For results of this investigation, the C_b factor is calculated by dividing the maximum moment at buckling by the moment capacity of the beam subjected to a uniform moment:

$$C_{b(ABAQUS)} = \frac{M_{cr(\text{moment gradient})}}{M_{cr(\text{uniform moment})}} \quad (4.5)$$

Here, the controlling C_b is used that resulted from treating either the top or bottom flange as the compression flange in the uniform moment case. The value of the $M_{cr(\text{moment gradient})}$ in Eq. (4.5) is the maximum moment within the unbraced length. Here, $M_{cr(\text{uniform moment})}$ is the moment at buckling in the flexural-torsional mode, while $M_{cr(\text{moment gradient})}$ is for distortional buckling of beam.

In the following figures (Figs 4.6 - 4.9), the moment modification factor $C_{b(ABAQUS)}$, which is based on distortional buckling, is compared with the C_b based on Eq. (4.1) and (4.2). As can be seen in almost all cases, SSRC Guidelines (1998) and Helwig et al (1997) give higher values of C_b . The deviation is too much for shorter beams. For $L/h \geq 8$, values of C_b are almost the same for all load cases. So, designing beams under reverse curvature bending (here a propped-cantilever beam) using SSRC guidelines and recommendations from Helwig et al (1997) may provide overestimated moment capacities in relatively short-beams.

Again, a comparison in results is shown in Figs. 4.10 & 4.11 for two beams of different lengths, $L/h = 6$ and 12. In these figures ABAQUS results for C_b based on lateral-torsional buckling analysis are also included. As expected, for a long beam ($L/h = 12$) there is very little difference in C_b whether one considers torsional buckling or distortional buckling in the beam. For a short span beam, $L/h = 6$, the difference in C_b values for torsional and distortional buckling is large.

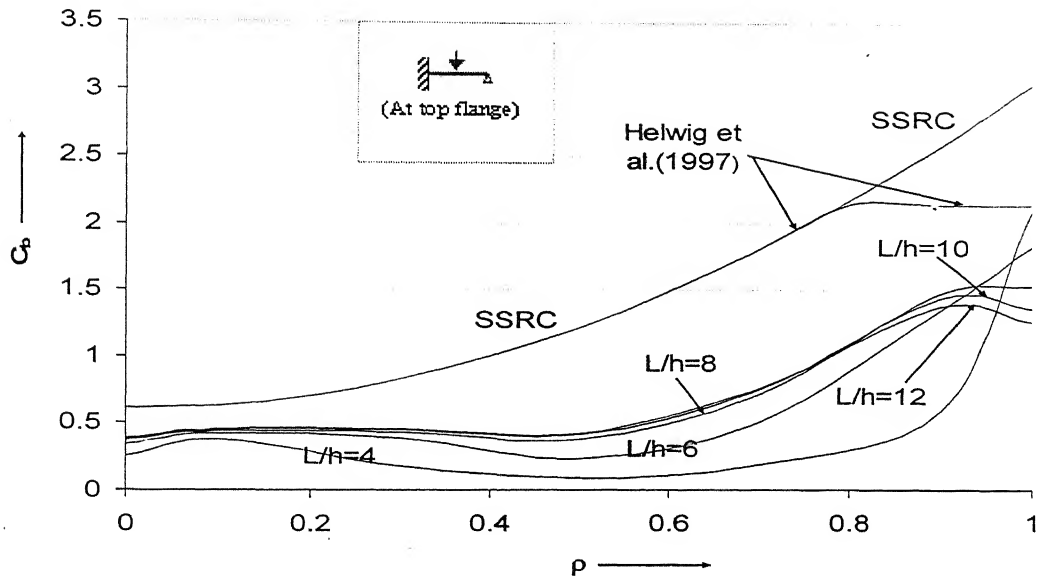


Fig 4.6: Comparison of Moment Modification Factors C_b with ρ :
Point Load at Top Flange [$\rho=0$: \perp , $\rho=0.5$: I , $\rho=1$: T]

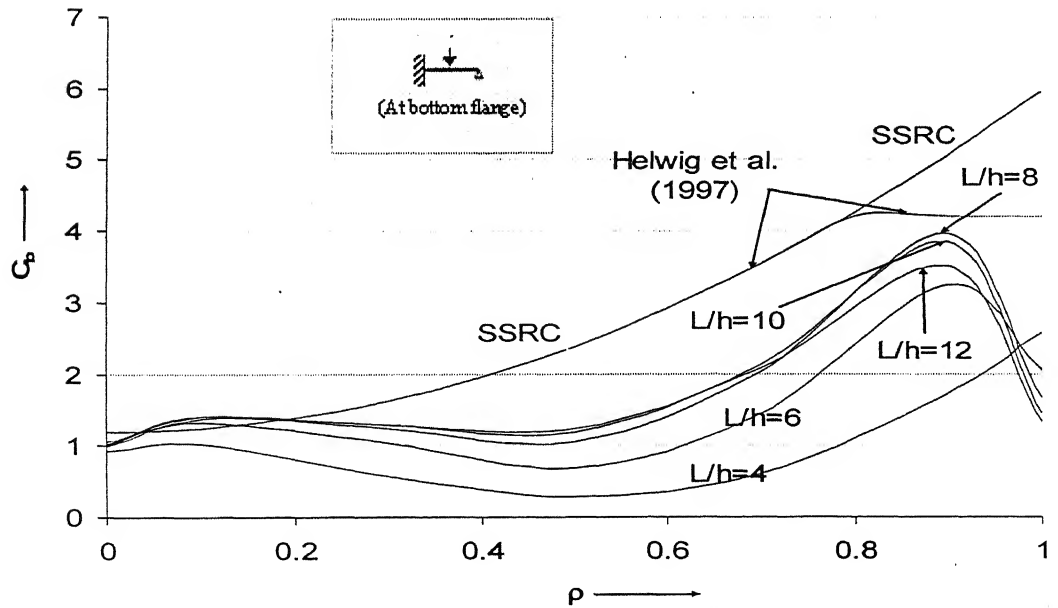


Fig 4.7: Comparison of Moment Modification Factors C_b with ρ :
Point Load at Bottom Flange [$\rho=0$: \perp , $\rho=0.5$: I , $\rho=1$: T]

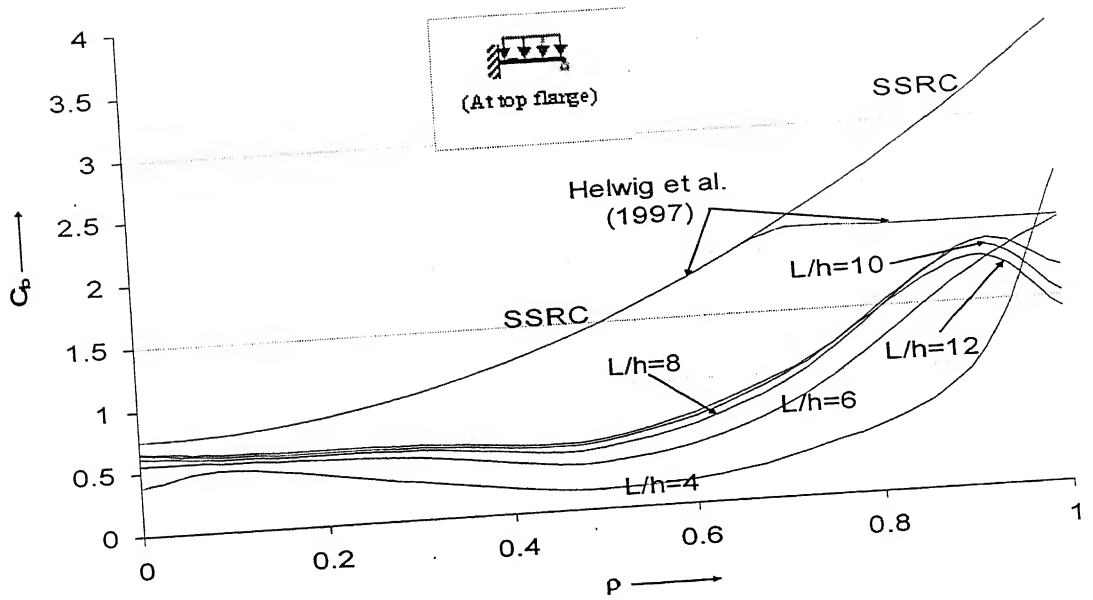


Fig 4.8: Comparison of Moment Modification Factors C_b with ρ :
UDL at Top Flange [$\rho=0$: \perp , $\rho=0.5$: I , $\rho=1$: T]

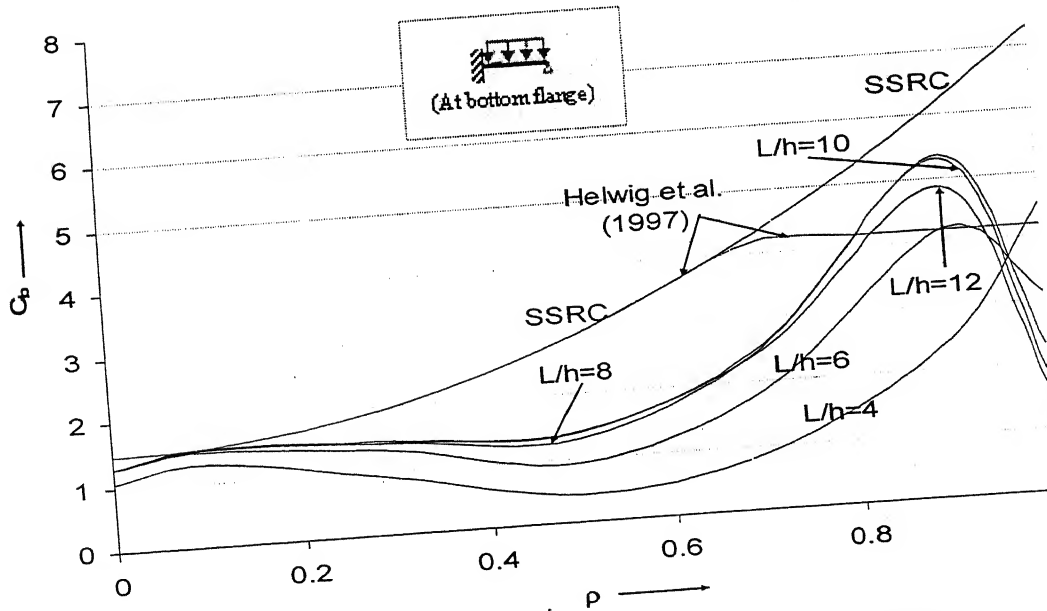


Fig 4.9: Comparison of Moment Modification Factors C_b with ρ :
UDL at Bottom Flange [$\rho=0$: \perp , $\rho=0.5$: I , $\rho=1$: T]

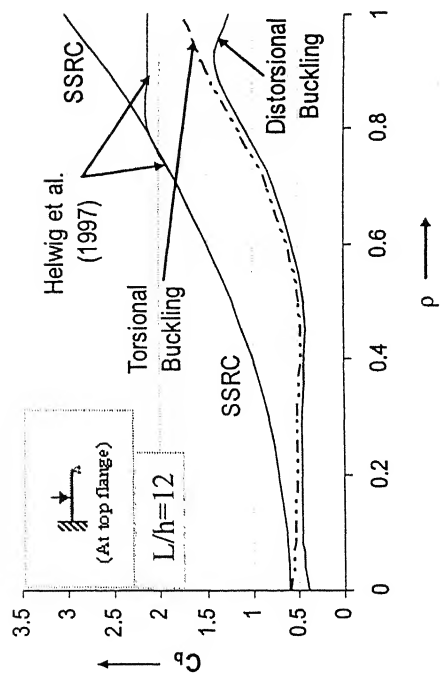


Fig 4.10a: Comparison of Moment Modification Factors C_b with ρ : Point Load at Top Flange ($L/h=12$)

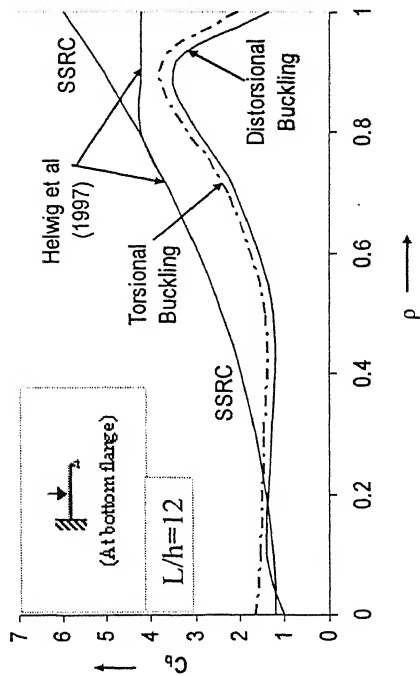


Fig 4.11a: Comparison of Moment Modification Factors C_b with ρ : Point Load at Bottom Flange ($L/h=12$)

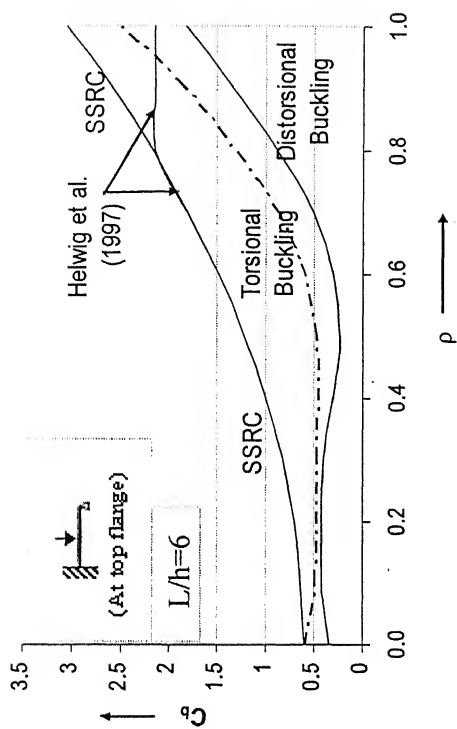


Fig 4.10b: Comparison of Moment Modification Factors C_b with ρ : Point Load at Top Flange ($L/h=6$)

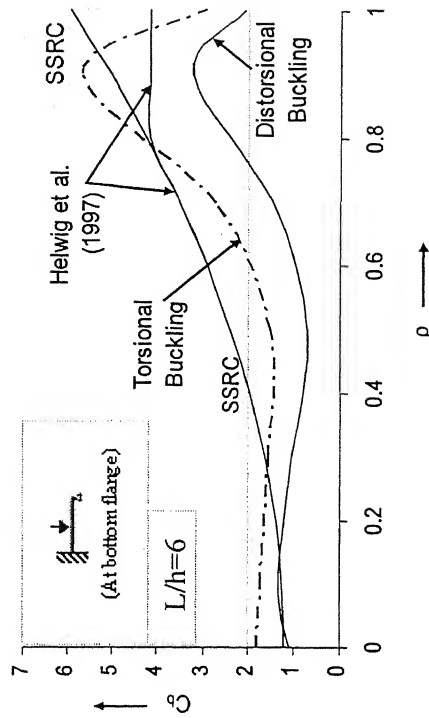


Fig 4.11b: Comparison of Moment Modification Factors C_b with ρ : Point Load at Bottom Flange ($L/h=6$)

4.5 Concluding Remarks

The buckling of beams (in the present case, a propped cantilever beam) subjected to reverse-curvature bending is more complex than the case of a single-curvature bending, because both of the flanges remain under compression at different locations along the beam length. As can be seen from the results presented in the previous sections, the available design specifications and solutions provide over-estimated values of moment modification factors for the two load cases considered. This deviation increases for short-length beams in which the distortional buckling is more predominant. So, while designing such beams, care should be taken for determining appropriate values of moment modification factors.

BRACED-CANTILEVER BEAMS

5.1 Introduction

Timoshenko and Gere (1961) obtained solutions for lateral torsional buckling of doubly-symmetric cantilever beams under uniform bending and suggested that the elastic critical moment M_{cr} can be given by

$$M_{cr} = \frac{\pi}{2L} (EI_y GJ)^{1/2} \left(1 + \frac{\pi^2 EI_w}{4GJL^2} \right)^{1/2} \quad (5.1)$$

where EI_y is the minor axis rigidity, GJ is the torsional rigidity and EI_w is the warping rigidity of the cantilever beam of length L . The above equation is identical to that for a simply supported beam under uniform bending; only the effective length L is replaced by $2L$. Nethercot (1983) provided a simple effective length method to get the critical moment M_{cr} :

$$M_{cr} = \frac{\pi}{K_{ef} L} (EI_y GJ)^{1/2} \left(1 + \frac{\pi^2 EI_w}{GJ(K_{ef} L)^2} \right)^{1/2} \quad (5.2)$$

where the K_{ef} is the effective length factor for various restraint conditions at the tip and at the root of the cantilever. Both end load and uniformly distributed load were considered. The Eq. (5.2) has also been included in SSRC Guidelines (1998) which provide the following values for K_{ef} :

Table 5.1: Table for Effective Length Factors (K_{ef})

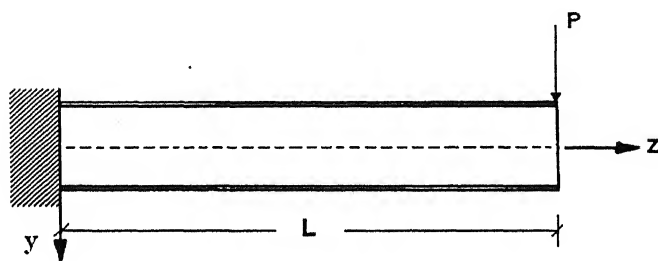
Restraint Conditions at Tip	Effective Length Factors (K_{ef})	
	Top Flange Loading	Bottom Flange Loading
Free (without brace)	1.4	0.8
Lateral brace at top flange	1.4	0.7
Lateral brace at top and bottom flange	0.6	0.6

There have been several subsequent studies on lateral buckling of cantilevers; some of these have also incorporated the effect of different types and positions of the lateral bracing. All these studies assumed that the cross-sections of the cantilever did not deform during buckling. However, it has been demonstrated that a beam under partial restraint at one of its ends may buckle in a distortional mode (Bradford 1988, 1990), for which the buckling load may be considerably lower than the load causing lateral-torsional buckling. So, it is important to consider the distortional buckling behaviour of such cantilever beams.

5.2 Present Study

Distortional buckling of cantilever I-beams is studied for three types of load (Fig 5.1); a point load at the tip, a uniformly distributed load and an end moment, for different degrees of mono-symmetry of beams. Top-flange and bottom-flange load positions are considered for the first two load cases. ABAQUS is used in the present investigation. The beam sections used are the same as given in Table 4.1 for the finite element modeling. The web thickness and the distance between flange centroids are kept constant, while the size of flanges is changed to vary the degree of beam monosymmetry property, ρ , from 0 to 1.0.

For the finite element modeling, the flanges and webs are modeled with S8R5 elements (*eight-node shell element with five degrees of freedom per node: three displacement components and two in-surface rotation components*). Eigenvalue analyses are conducted to determine buckling loads. The Young's modulus E is taken as 206.6 GPa and Poisson's ratio ν is as 0.3.



Point Load at Tip

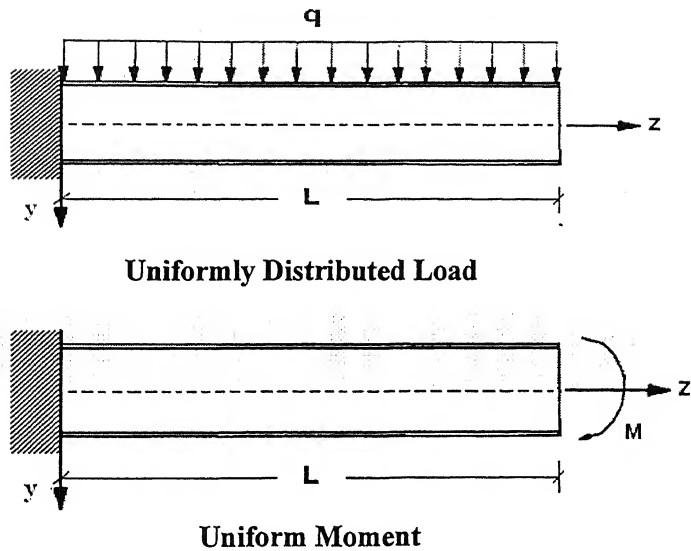


Fig. 5.1 Load Cases Considered

Three types of lateral bracing are considered along the span of the cantilever beam: (a) lateral translational bracing at top flange only, (b) lateral translational bracing at bottom flange only, (c) lateral translational bracing at top & bottom flanges. These are shown in Fig. 5.2.

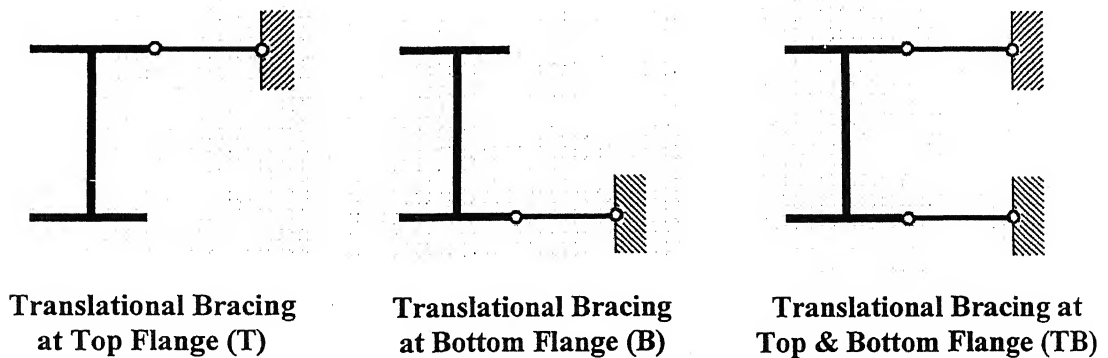


Fig. 5.2 Types of Bracing

5.3 Comparison with Results of Kitipornchai et al (1984, 1987)

Kitipornchai et al (1984) performed experimental investigation on high strength aluminium cantilever I-beams. A doubly-symmetric beam section was taken with overall depth 75.2mm, thickness of flanges 3.1mm, width of flanges 31.4mm, thickness of web

2.0mm. The length of the beam varied from 1m to 3m. The load was applied as close to the tip as practically possible. They also compared the experimental buckling loads with their own analytical results based on the finite integral approach. Later, Wang et al. (1987) compared these results with the finite element and the energy method. Table 5.2 shows this comparison along with the results which are obtained using ABAQUS that takes into account distortional buckling of the cantilever beam using three types of brace at the tip of the cantilever: top translational bracing, bottom translational bracing (shown in Fig. 5.2), and full restraints bracings (lateral & rotational brace at top and bottom flange). Only top flange loading is considered here for the comparison.

The present ABAQUS results match closely with the comparisons given in Wang et al (1987) and Kitipornchai et al. (1984) in spite of the fact that the former take into account the effect of distortional buckling. The reason for such a close match is that the beams considered are the long ones (the sectional dimensions of the experimental beam are such that the L/h ratio varies from about 13 to 40) and buckle in the lateral-torsional mode only. On the other hand, even for such long beams, SSRC Guidelines (based on Eq.5.2 and Table 5.1) provide a very conservative estimate of the buckling load.

Table 5.2: Comparison of Results

Beam Length (m)	Type of Bracing	Buckling Load (N)					
		Experiment (Kitipornchai et al., 1984)	Finite Integral (Kitipornchai et al., 1984)	Finite Element (Wang et al., 1987)	Energy (Wang et al., 1987)	SSRC Guidelines (1998)	Present Study (ABAQUS)
3	F	181.5	188.3	189.6	190.2	-	187.17
3	T	104	112.7	114	114	37.6	113.36
3	B	80.4	85	87.7	87.4	-	87.03
1.5	F	803.3	902.5	914.5	918.8	-	885.71
1.5	T	382	424.8	441.1	440.3	157.9	428.28
1.5	B	294	282.2	291.8	290.8	-	283.50
1	T	750.5	801.8	-	-	382.1	886.25
1	B	519.9	520.2	-	-	-	563.95

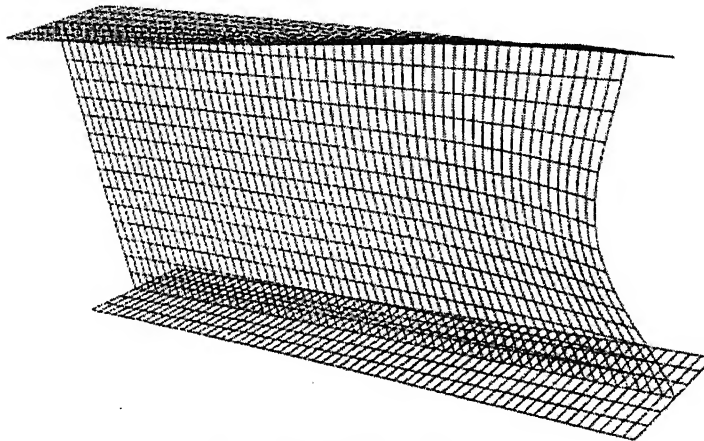
T: Lateral brace at top flange only

B: Lateral brace at bottom flange only

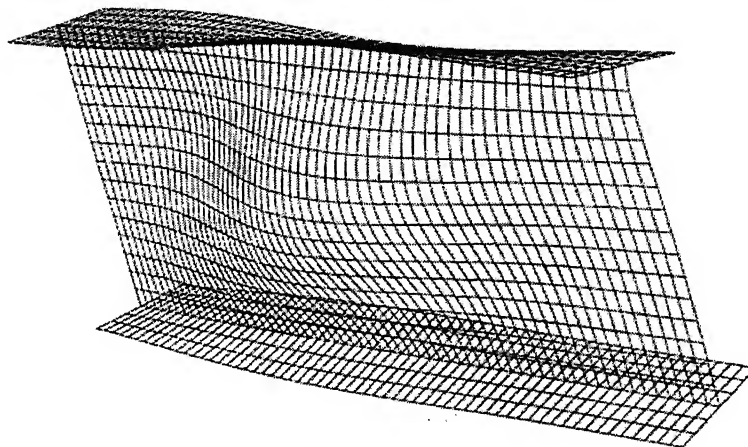
F: Full brace (Lateral & rotational brace at top flange and bottom flange)

5.4 Buckling Loads

First, using ABAQUS, the buckled shapes of the cantilever beam of doubly-symmetric section ($\rho = 0.5$) are obtained when it is subjected to a point load at the free-end on the top/bottom flange. These are shown in Fig. 5.3 (for $L/h = 2$) and in Fig. 5.4 (for $L/h = 5.33$). As can be seen in these figures, the effect of distortional buckling is much more in the short beam ($L/h = 2$) but for the longer beam ($L/h = 5.33$) the effect of distortional buckling is very less and the beam practically buckles in lateral-torsional mode. Therefore in what follows, the buckling loads are obtained for the above range of L/h only for different brace locations and for various degrees of beam monosymmetry.

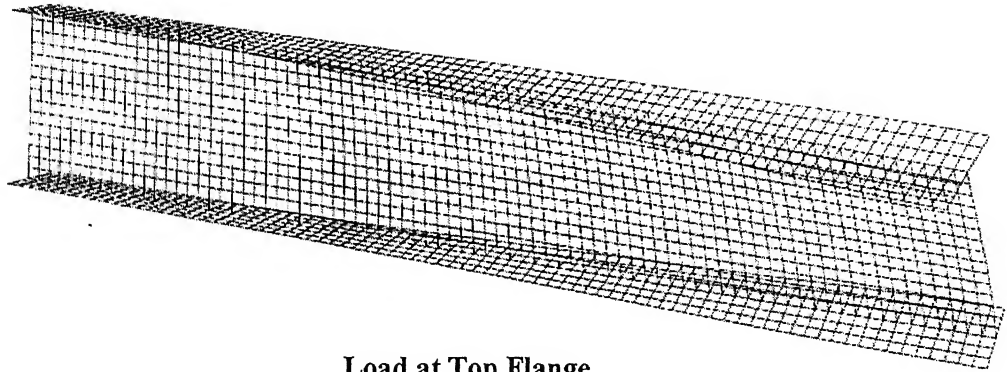


Load at Top Flange

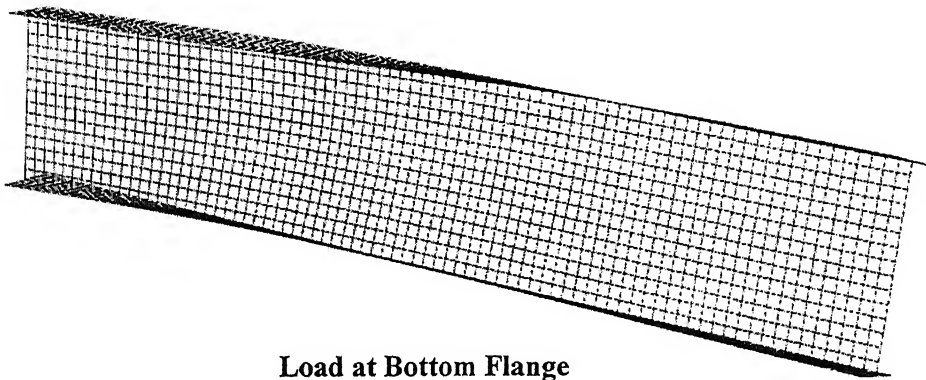


Load at Bottom Flange

Fig. 5.3 Buckled Shape in Cantilever Beam ($L/h = 2$):
Point Load at Free End



Load at Top Flange



Load at Bottom Flange

**Fig. 5.4 Buckled Shape in Cantilever Beam ($L/h = 5.33$):
Point Load at Free End**

At first two doubly-symmetric beams: one of relatively short length (1.2m, $L/h=2$) and other of relatively larger length (3.2m, $L/h=5.33$) are taken for investigation under point and uniformly distributed loads. The objective is to study the effect of the type and the location of brace on the buckling load. Results are shown in Figs. 5.5 – 5.12. For the short beam, in case of top flange point load (Fig. 5.5) or top flange uniformly distributed load (udl) (Fig. 5.6), the buckling load is almost the same for top flange lateral bracing (T-bracing) as well as bottom flange lateral bracing (B-bracing). Lateral bracing provided simultaneously at top and bottom flanges (TB-bracing) helps very little in increasing the buckling load for top flange loadings (Fig. 5.5 & Fig. 5.6). In case of the bottom flange loadings, the buckling load is higher for B-bracing than for T-bracing and is much higher for TB-bracing (Fig. 5.7 & Fig. 5.8). The effectiveness of bracing is highest when it is located at about $0.75L$ from the fixed end in the case of point load and at about $0.4L$ from the fixed end in the case of udl.

In the long beam, and for top flange loadings (Fig. 5.9 & Fig. 5.10), the T-bracing yields higher buckling load than the B-bracing. The TB-bracing increases the buckling capacity of the beam to a very large extent; the effect of bracing is more pronounced at the tip of the beam for the point load (Fig. 5.9) and at about $0.7L$ from the fixed end for the udl (Fig. 5.10). In case the of bottom flange loadings (Figs 5.11, 5.12), generally, the T-bracing is more effective than the B-bracing. The TB-bracing is much more effective only at about $0.4L$ from the fixed end.

A similar investigation for the case of a uniform moment reveals that the T-bracing & the B-bracing have very little effect on the buckling moment of short and long beams (Fig. 5.13 & Fig. 5.14). On the other hand, the TB-bracing does increase the buckling capacity of the longer beam specially if the bracings are positioned towards the free end (Fig. 5.14).

Next objective is to study the effect of positioning of different bracings on a cantilever beam of fixed length ($L=2m$, $L/h=3.33$) for sections having different degrees of monosymmetry; ρ varies from 0 to 1.0. Again, a point load and a udl are taken and placed either at the top flange or the bottom flange. All results are shown in Fig. 5.15 – 5.26.

T-bracing

For the top flange loadings, the trend in buckling load is similar for both load cases (Fig. 5.15 & Fig. 5.16) except for $\rho = 0$. For $\rho = 0$, T-bracing helps most when placed at the free end for the point load and at about $0.8L$ from the fixed end for the udl. When $\rho = 1$ (the T-section beam), the location of the T-bracing has no effect on the buckling capacity of the beam. In general, a larger bottom flange helps in increasing the buckling capacity.

For bottom flange loadings the position of bracing has practically no effect on a beam of given section (Fig. 5.17 & Fig. 5.18). Generally, a larger bottom flange helps in increasing the buckling capacity of the beam.

B-bracing

A larger top flange helps in increasing the buckling capacity of the beam except for $\rho = 1$, for both load cases (Fig. 5.19 & Fig. 5.20) placed at the top flange. For $\rho = 0$, bracings practically have no effect on the buckling capacity. For $\rho = 0.3, 0.5, 0.7$ the

increase in buckling load is maximum when the bracing is towards the free-end (in case of point load) and at about $0.7L$ from the fixed end for the udl.

For bottom flange loadings (Fig. 5.21 & Fig. 5.22) a larger bottom flange helps in increasing the buckling capacity of the beam. The bracing practically does not help in increasing the buckling capacity except for $\rho = 0$, where the effect is beneficial when the beam is braced towards the free end.

TB-bracing

For both top flange loadings, the trend in variation in buckling loads is similar for the point load (Fig. 5.23) and for the udl (Fig. 5.24) except for $\rho = 0$. For $\rho = 0$, the bracing is more effective at the tip for the point load and at about $0.8L$ from the fixed end for the udl. For $\rho = 1$, the bracing is almost ineffective in both cases.

In case of bottom flange loadings, the bracing is more effective for beams having larger bottom flange, like an inverted T-section beam (Fig. 5.25 & Fig. 5.26). For $\rho = 0$, the bracing is more effective at the tip for the point loading and beyond $0.2L$ from the fixed end for the udl. T-sections ($\rho = 1.0$) are most ineffective for both load cases.

Uniform Moment

Results for the case of a uniform moment are shown in Figs. 5.27 - 5.29. The T-bracing is more effective for beam sections with larger bottom flange, and has no effect in increasing the buckling capacity of the beam having a T-section ($\rho = 1.0$). The B-bracing is effective for sections with $\rho = 0.3-0.7$ when it is placed near the free end of the cantilever. For $\rho = 1$, it is more effective when placed at about $0.8L$ from the fixed end. The inverted T-sections ($\rho = 0$) remain unaffected from the positioning of the B-brace. The TB-bracing increases the buckling capacity of the beam considerably when placed at about $0.85L$ from the fixed end for $\rho = 0$. Beam sections with larger bottom flanges are desirable. This kind of bracing is more desirable towards the tip of the beam for $\rho = 0.3, 0.5, 0.7$. For T-sections ($\rho = 1.0$), bracings are effective at about $0.8L$ from the fixed end of the cantilever.

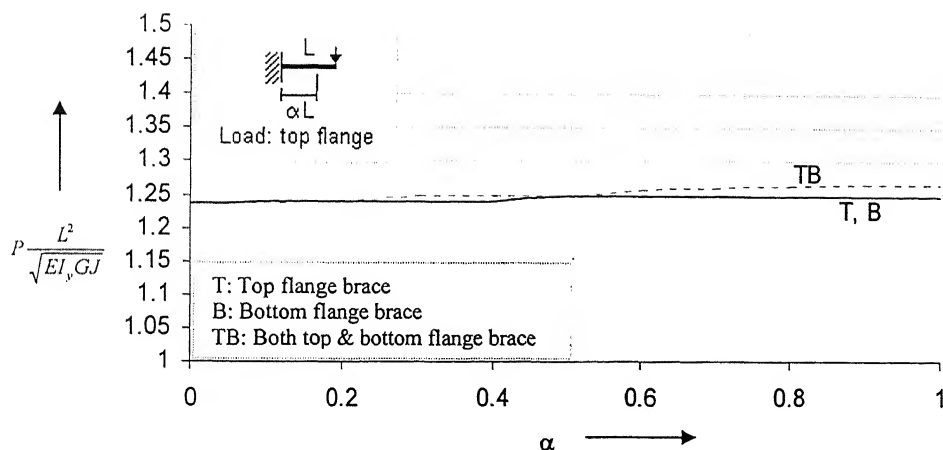


Fig. 5.5 Variations in Buckling Loads with Location of Different Types of Lateral Brace: Point Load at Top Flange ($L/h=2$, $\rho=0.5$)

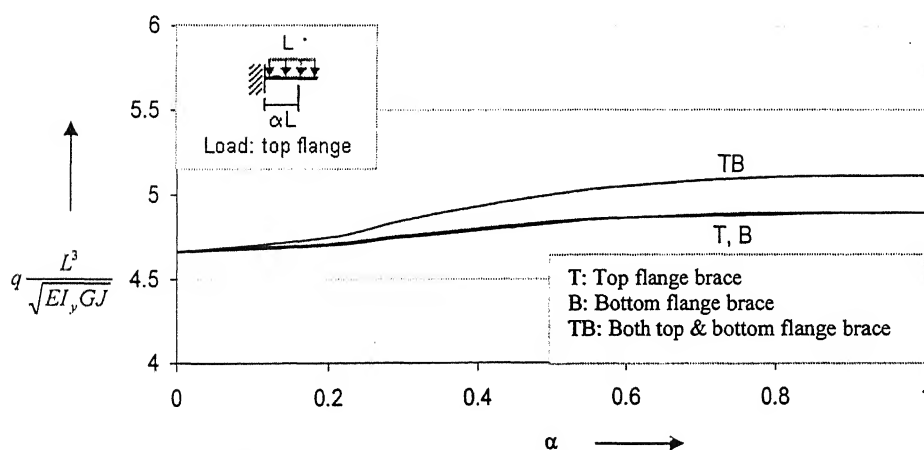


Fig. 5.6 Variations in Buckling Loads with Location of Different Types of Lateral Brace: UDL at Top Flange ($L/h=2$, $\rho=0.5$)

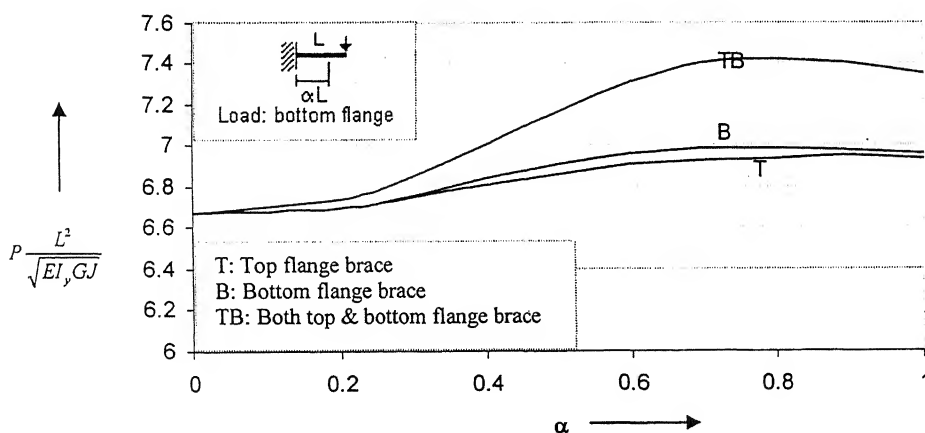


Fig. 5.7 Variations in Buckling Loads with Location of Different Types of Lateral Brace: Point Load at Bottom Flange ($L/h=2$, $\rho=0.5$)

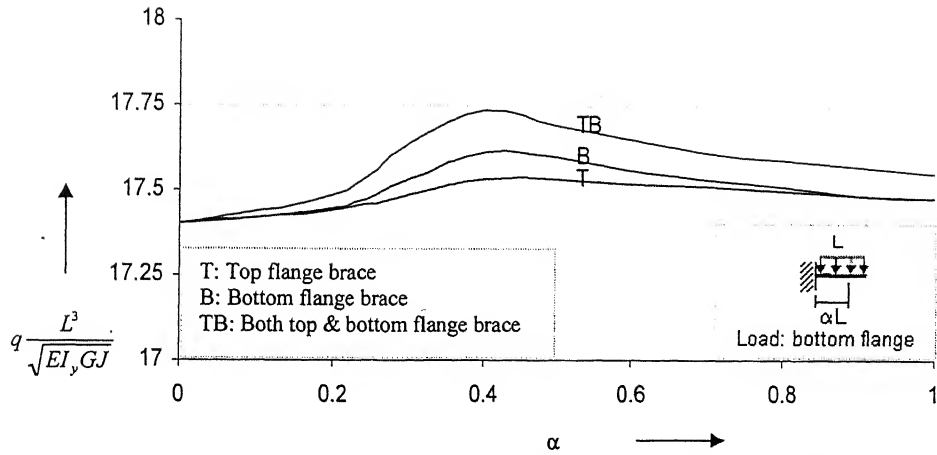


Fig. 5.8 Variations in Buckling Loads with Location of Different Types of Lateral Brace: *UDL at Bottom Flange* ($L/h=2$, $\rho=0.5$)

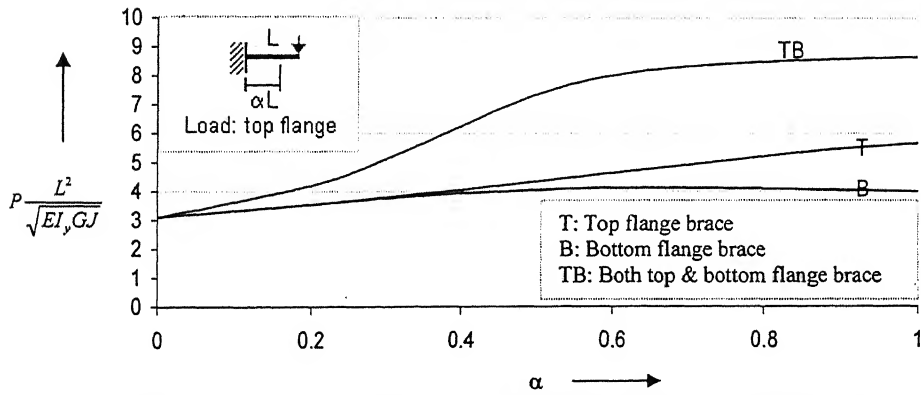


Fig. 5.9 Variations in Buckling Loads with Location of Different Types of Lateral Brace: *Point Load at Top Flange* ($L/h=5.33$, $\rho=0.5$)

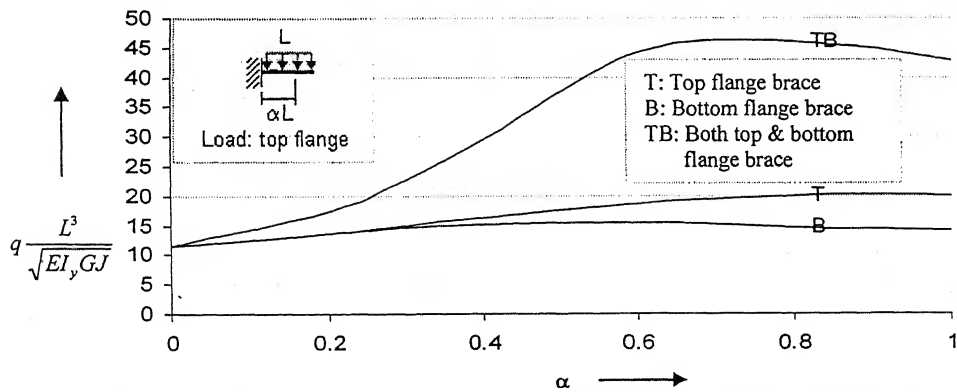


Fig. 5.10 Variations in Buckling Loads with Location of Different Types of Lateral Brace: *UDL at Top Flange* ($L/h=5.33$, $\rho=0.5$)

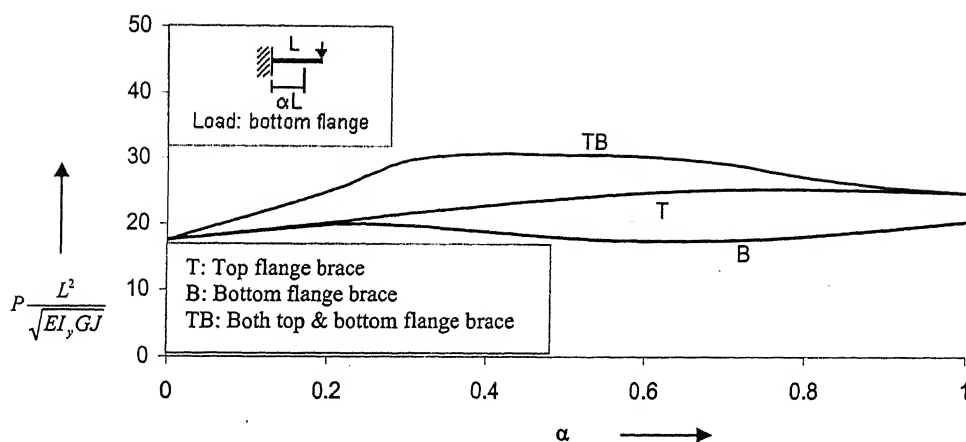


Fig. 5.11 Variations in Buckling Loads with Location of Different Types of Lateral Brace: Point Load at Bottom Flange ($L/h=5.33$, $\rho=0.5$)

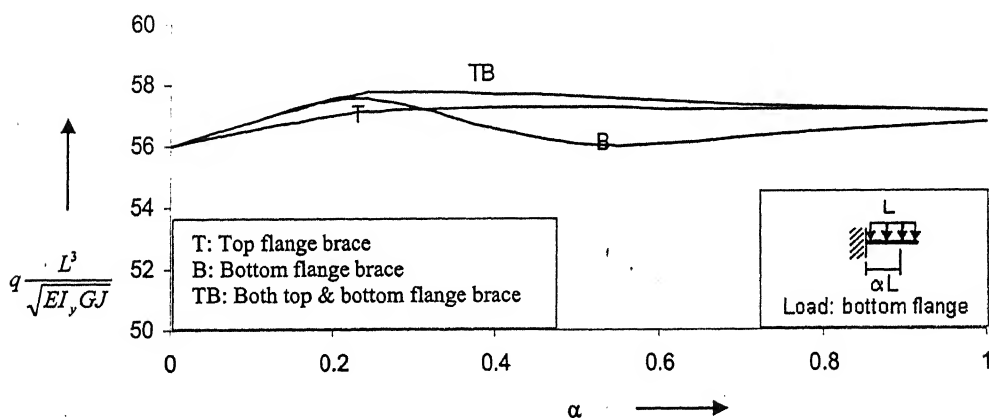


Fig. 5.12 Variations in Buckling Loads with Location of Different Types of Lateral Brace: UDL at Bottom Flange ($L/h=5.33$, $\rho=0.5$)

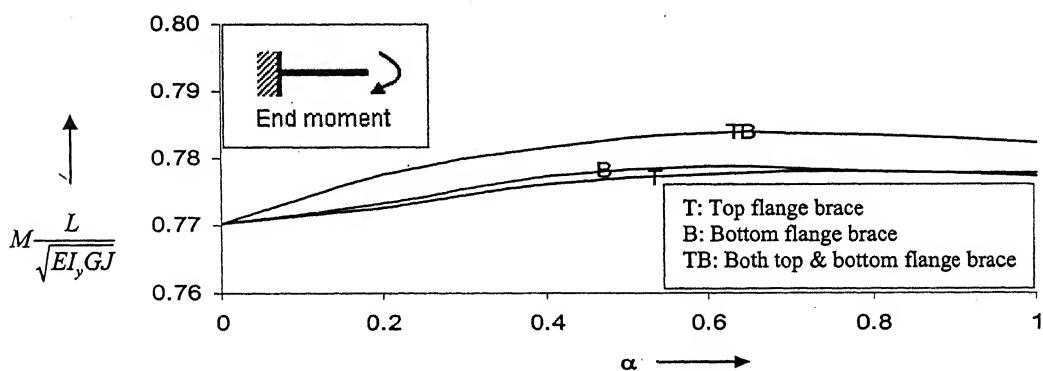


Fig. 5.13 Variations in Buckling Loads with Location of Different Types of Lateral Brace: End Moment ($L/h=2$, $\rho=0.5$)

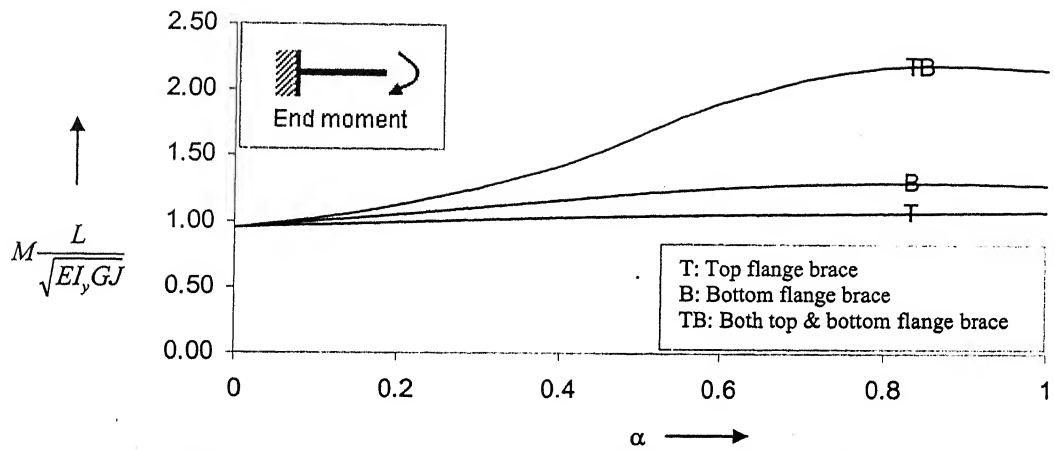


Fig. 5.14 Variations in Buckling Loads with Location of Different Types of Lateral Brace: *End Moment* ($L/h=5.33$, $\rho=0.5$)

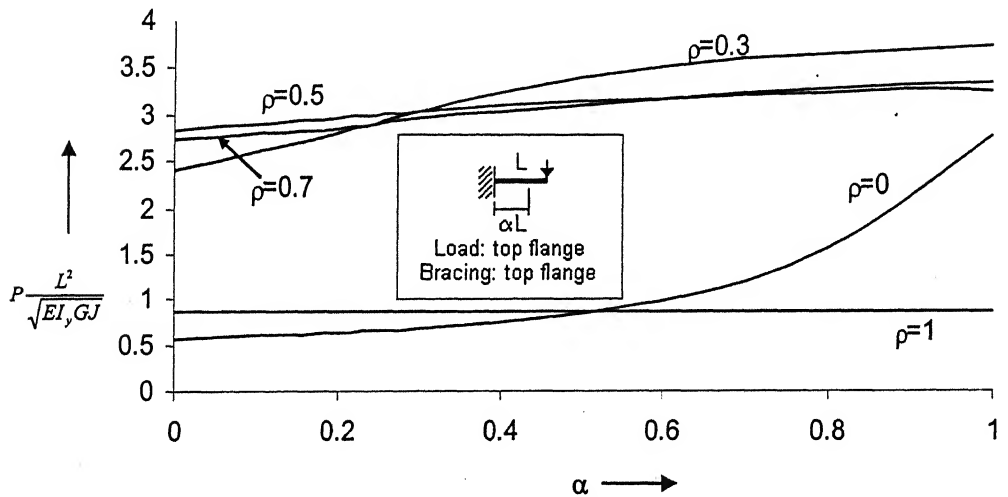


Fig. 5.15 Variations in Buckling Loads with Location of Lateral Brace: *Point Load at Top Flange, Bracing at Top Flange* ($L=2m$)

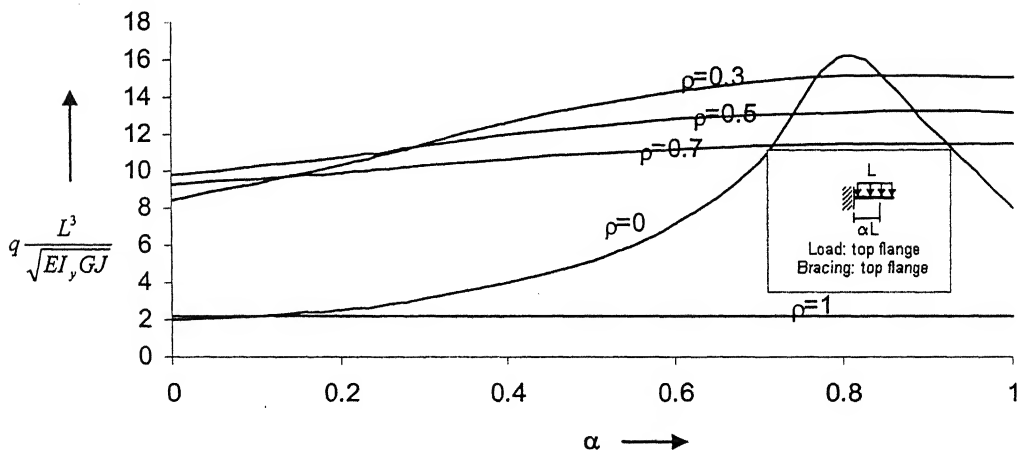


Fig. 5.16 Variations in Buckling Loads with Location of Lateral Brace: *UDL at Top Flange, Bracing at Top Flange* ($L=2m$)

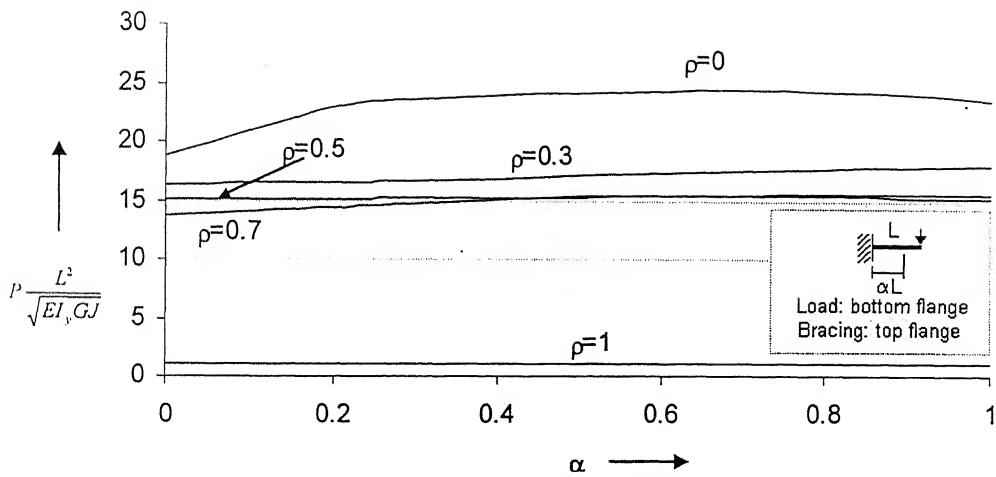


Fig. 5.17 Variations in Buckling Loads with Location of Lateral Brace: Point Load at Bottom Flange, Bracing at Top Flange ($L=2m$)

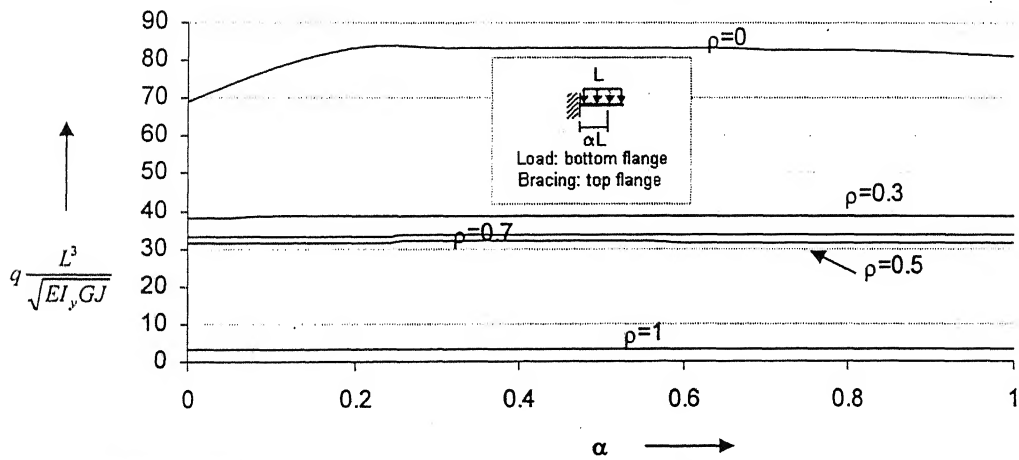


Fig. 5.18 Variations in Buckling Loads with Location of Lateral Brace: UDL at Bottom Flange, Bracing at Top Flange ($L=2m$)

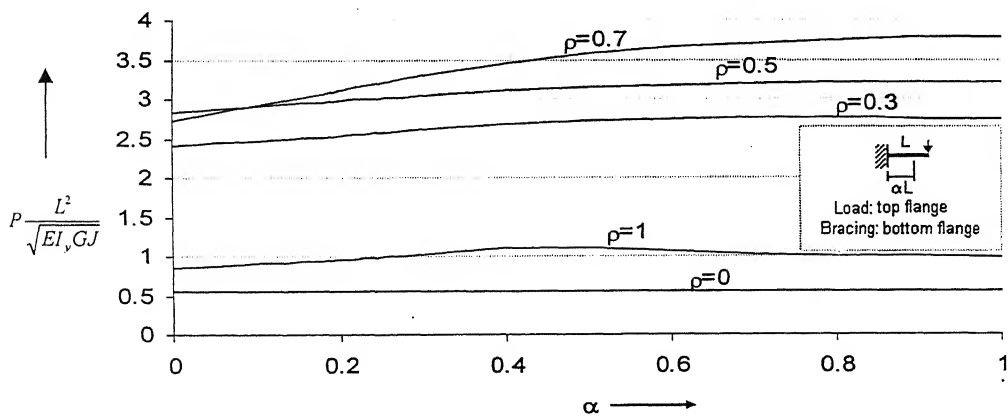


Fig. 5.19 Variations in Buckling Loads with Location of Lateral Brace: Point Load at Top Flange, Bracing at Bottom Flange ($L=2m$)

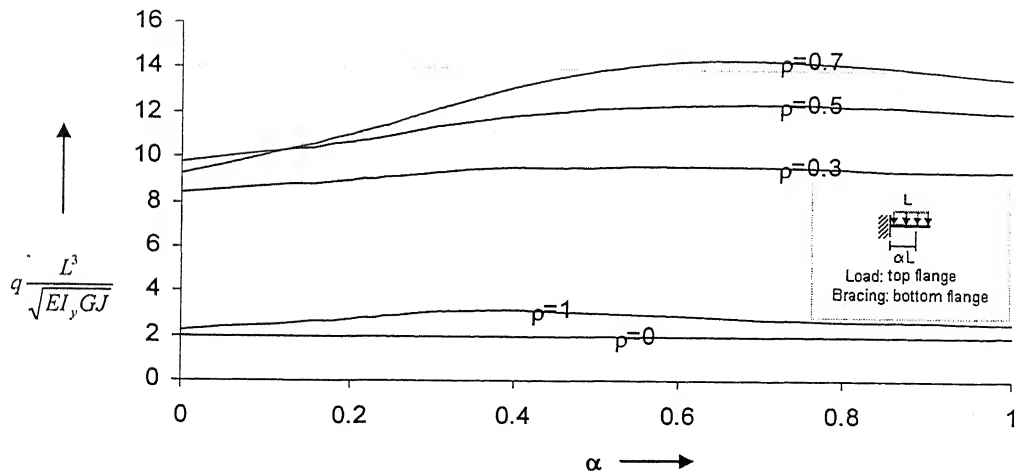


Fig. 5.20 Variations in Buckling Loads with Location of Lateral Brace: UDL at Top Flange, Bracing at Bottom Flange (L=2m)

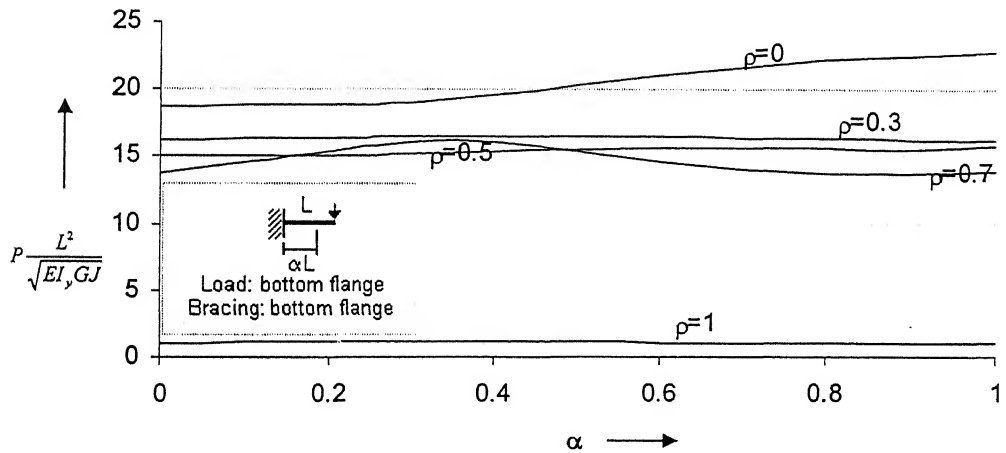


Fig. 5.21 Variations in Buckling Loads with Location of Lateral Brace: Point Load at Bottom Flange, Bracing at Bottom Flange (L=2m)

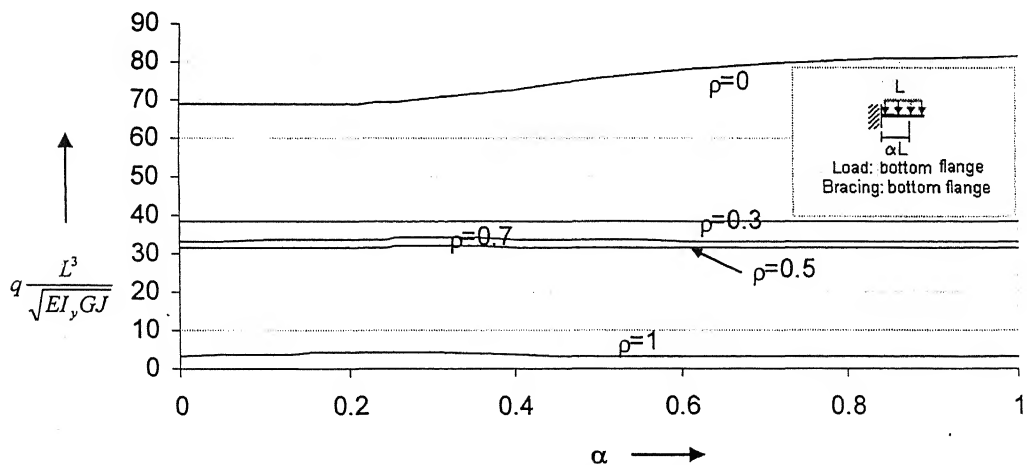


Fig. 5.22 Variations in Buckling Loads with Location of Lateral Brace: UDL at Bottom Flange, Bracing at Bottom Flange (L=2m)

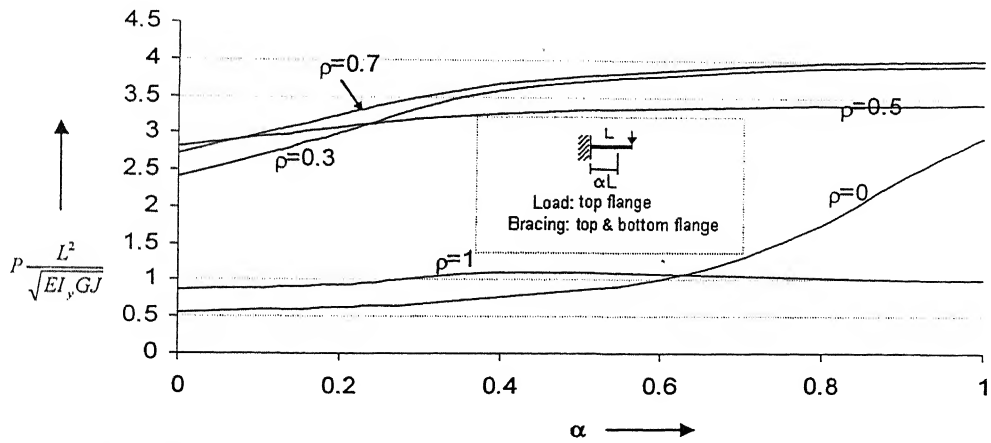


Fig. 5.23 Variations in Buckling Loads with Location of Lateral Brace: Point Load at Top Flange, Bracing at Top & Bottom Flange ($L=2m$)

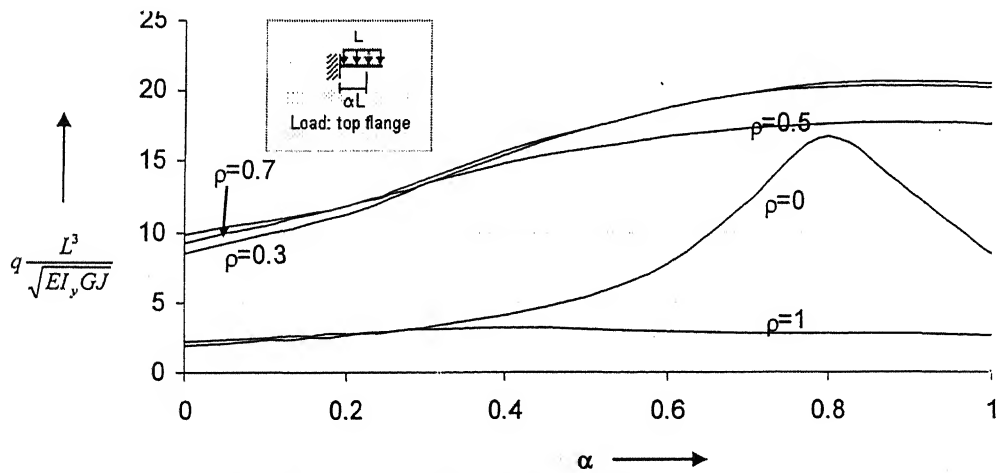


Fig. 5.24 Variations in Buckling Loads with Location of Lateral Brace: UDL at Top Flange, Bracing at Top & Bottom Flange ($L=2m$)

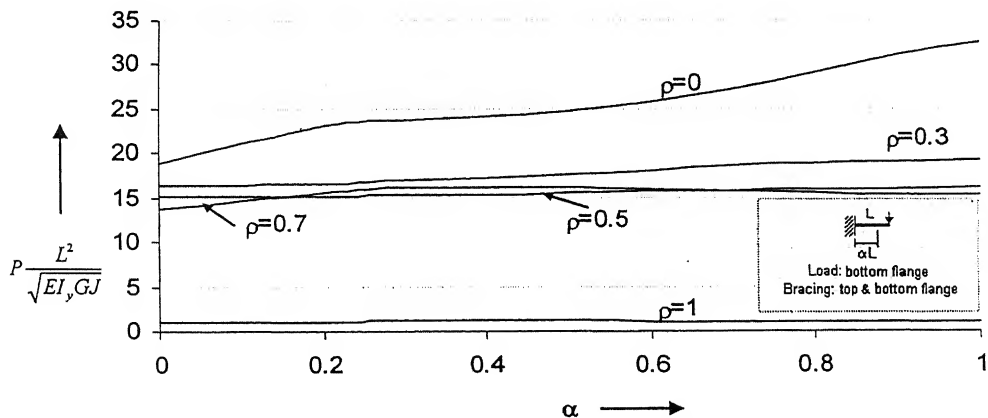


Fig. 5.25 Variations in Buckling Loads with Location of Lateral Brace: Point Load at Bottom Flange, Bracing at Top & Bottom Flange ($L=2m$)

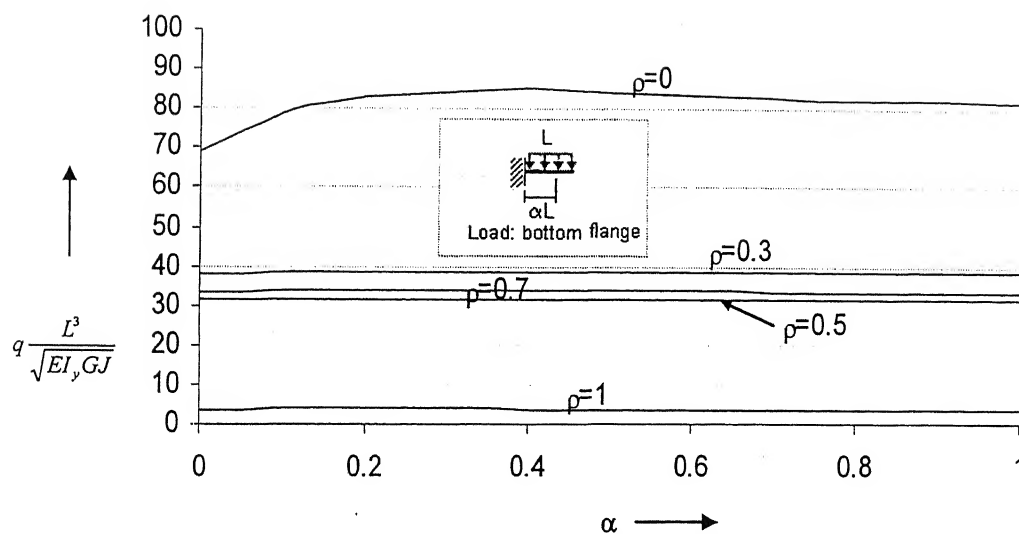


Fig. 5.26 Variations in Buckling Loads with Location of Lateral Brace: UDL at Bottom Flange, Bracing at Top & Bottom Flange ($L=2m$)

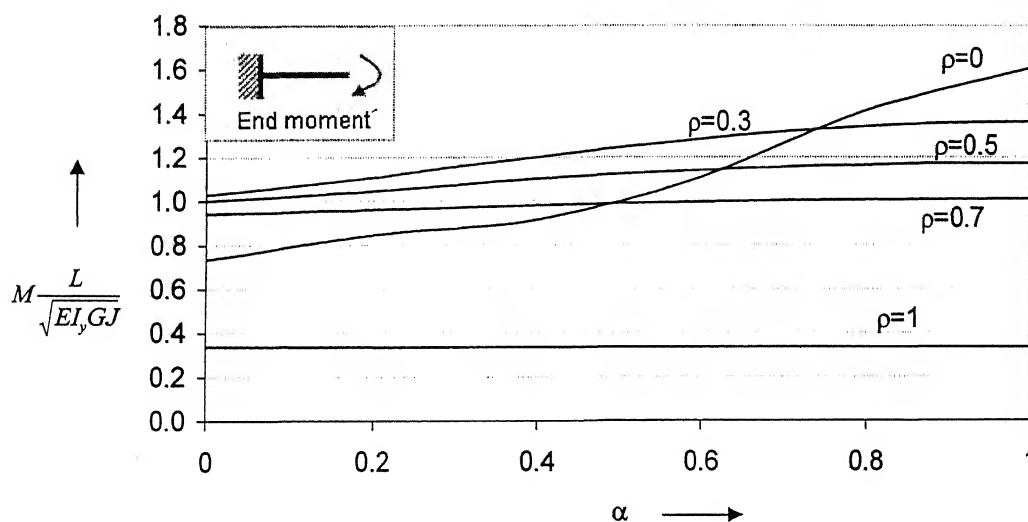


Fig. 5.27 Variations in Buckling Loads with Location of Lateral Brace: Uniform Moment, Bracing at Top Flange ($L=2m$)

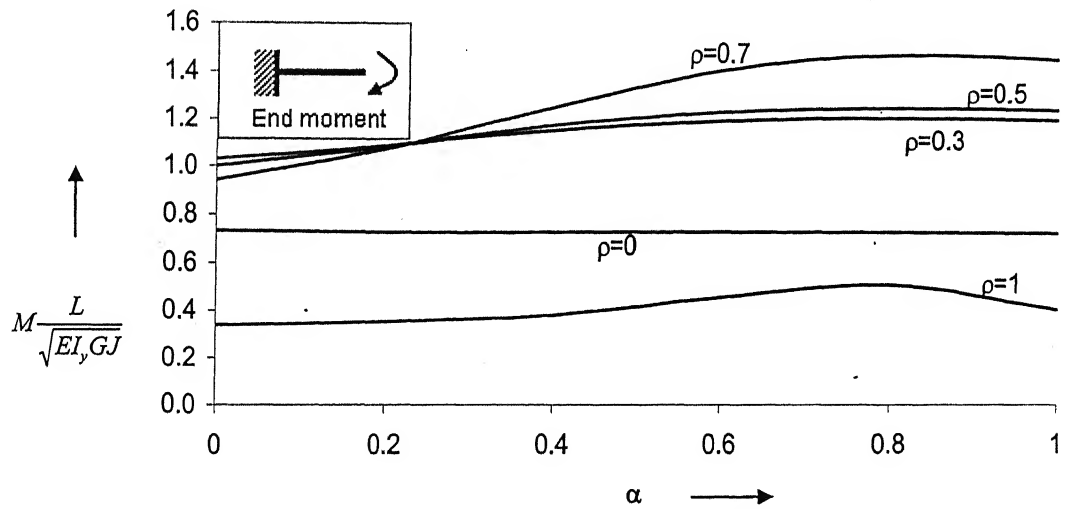


Fig. 5.28 Variations in Buckling Loads with Location of Lateral Brace: *End Moment, Bracing at Bottom Flange* ($L=2m$)

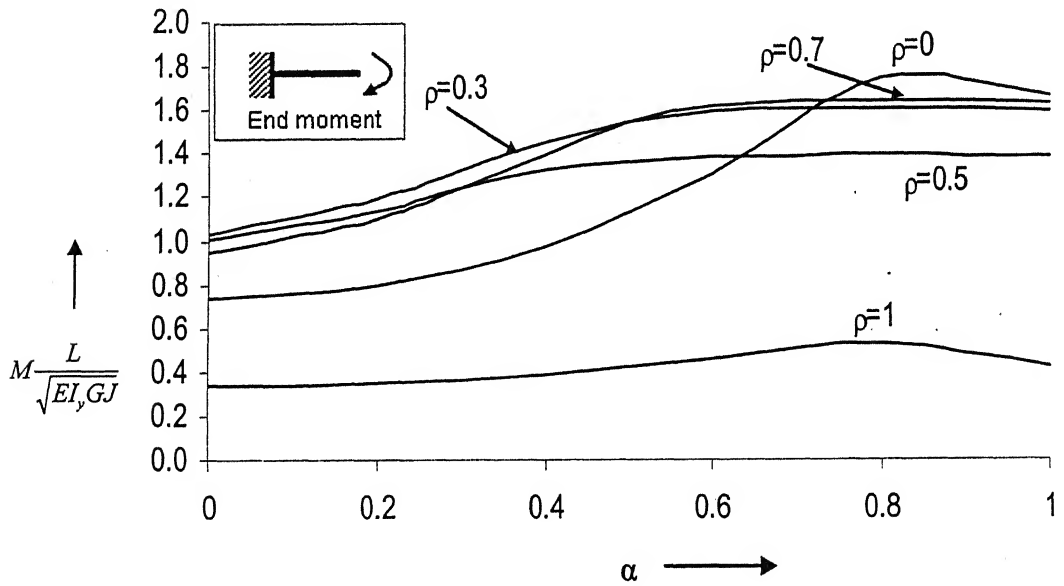


Fig. 5.29 Variations in Buckling Loads with Location of Lateral Brace: *End Moment, Bracing at Top & Bottom Flange* ($L=2m$)

5.5 Comparison with SSRC Guidelines

Buckling loads for the beam of length 2m ($L/h=3.33$) and for $\rho = 0.3, 0.5, 0.7$ are compared with those obtained using SSRC Guidelines which are based on Eq. (5.2) and Table 5.1. The comparison is given in Table 5.3. It is very difficult to draw any definite conclusion in the absence of a specific trend. In some cases, the two results are even comparable, but this raises doubt in the applicability of SSRC Guidelines since for long beams (which buckle in lateral torsional mode) these guidelines provided very conservative values of buckling loads (Table 5.2).

Table 5.3: Comparison with SSRC Guidelines for $L=2m$ ($L/h=3.33$):

$\rho=0.7$

A. Without Bracing

Load	Top flange loading		Bottom flange loading	
	SSRC	ABAQUS	SSRC	ABAQUS
Point Load (N)	882553	502467	2496197	2530760
UDL (N/m)	882553	849657	2496197	3053190

B. Top-lateral Bracing

Load	Top flange loading		Bottom flange loading	
	SSRC	ABAQUS	SSRC	ABAQUS
Point Load (N)	882553	621284	3228245	2810100
UDL (N/m)	882553	1053800	3228245	3076030

C. Top & bottom-lateral Bracing

Load	Top flange loading		Bottom flange loading	
	SSRC	ABAQUS	SSRC	ABAQUS
Point Load (N)	4355786	7389260	4355786	2811311
UDL (N/m)	4355786	1891960	4355786	3077140

$\rho = 0.5$

A. Without Bracing

Load	Top flange loading		Bottom flange loading	
	SSRC	ABAQUS	SSRC	ABAQUS
Point Load (N)	1298009	607012	3786261	3243950
UDL (N/m)	1298009	1046285	3786261	3394905

B. Top-lateral Bracing

Load	Top flange loading		Bottom flange loading	
	SSRC	ABAQUS	SSRC	ABAQUS
Point Load (N)	1298009	703600	4916502	3357840
UDL (N/m)	1298009	1413660	4916502	3404520

C. Top & bottom-lateral Bracing

Load	Top flange loading		Bottom flange loading	
	SSRC	ABAQUS	SSRC	ABAQUS
Point Load (N)	6657722	734008	6657722	3452840
UDL (N/m)	6657722	1904150	6657722	3406110

$$\rho = 0.3$$

A. Without Bracing

Load	Top flange loading		Bottom flange loading	
	SSRC	ABAQUS	SSRC	ABAQUS
Point Load (N)	882553	442819	2496197	2997800
UDL (N/m)	882553	775123	2496197	3516570

B. Top-lateral Bracing

Load	Top flange loading		Bottom flange loading	
	SSRC	ABAQUS	SSRC	ABAQUS
Point Load (N)	882553	693407	3228245	3310490
UDL (N/m)	882553	1386430	3228245	3540720

C. Top & bottom-lateral Bracing

Load	Top flange loading		Bottom flange loading	
	SSRC	ABAQUS	SSRC	ABAQUS
Point Load (N)	4355786	725491	4355786	3539780
UDL (N/m)	4355786	1868730	4355786	3543630

5.6 Concluding Remarks

Except for the T-section or the inverted T-section cantilever beams, top lateral bracings are very effective for beam sections having larger bottom flanges when a point load or a uniformly distributed load acts at the top flange, and for the uniform moment

case. On the other hand, bottom lateral bracings are very effective for beam sections having larger top flanges. When loads are placed at the bottom flange, the position of any kind of lateral bracing has practically no effect on the buckling capacity of a monosymmetric cantilever beam, except for $\rho = 0$.

SUMMARY AND CONCLUSIONS

6.1 Summary

There have been two main considerations in this thesis: first a comparison of different code specifications for the lateral-torsional buckling analysis of monosymmetric I-beams and secondly, a study of distortional buckling in beams using ABAQUS. Comparison of relevant code specifications (IS: 800 (1984) specifications, Revised IS: 800 (Draft) specifications, LRFD Specifications, SSRC Guidelines) has been done for simply supported beams only. For the finite element analysis using ABAQUS, three types of monosymmetric beam: simply supported beam, propped-cantilever beam, and braced cantilever beam have been considered. The analysis has been performed by considering three types of load: a point load, a uniformly distributed load and uniform moment. Both the top and bottom flange loadings have been considered for the first two types of load. In order to take into account distortional buckling, quadratic shell elements have been used to model the beam sections which consider small strains but large rotations. Keeping the depth and the thickness of the web and the width and the thickness of one flange fixed, the width and the thickness of the other flange has been changed to vary the degree of monosymmetry of the beam. Eigenvalue analyses have been performed to determine the buckling loads. In addition, wherever possible the results have been compared with different code specifications or with those available in literature. For simply supported and propped cantilever beams, moment modification factors have been calculated and compared with the provisions given in SSRC Guidelines. For braced cantilever beams, the effect of different types of brace (i.e. lateral translational bracing at top flange only, lateral translational bracing at bottom flange only, lateral translational bracing at top & bottom flanges) and their positions along the beam have been investigated to find out the most effective bracing type and its location.

6.2 Conclusions

IS: 800 (1984) specifications use Merchant-Rankine formula and suggest the use of elastic flexural-torsional buckling analysis for the design of steel I-beams. While these specifications prove useful for simply supported monosymmetric I-beams subjected to a constant moment, for other load cases they may provide underestimated / overestimated values of design stress. The code IS: 800 is under revision and the available revised draft specifications do include solutions for different load cases and load positions. The SSRC Guidelines have suggested a simple moment modification factor technique which can be used for different types of load and load positions. These, however are based on flexural-torsional buckling analysis.

A general observation based on the present investigation is that the distortional buckling has a significant effect on short length beams, at least for the types of beam considered. For simply supported beams it is seen that for a uniform moment case, the difference between the flexural-torsional buckling moment and the distortional buckling moment is very less, even for short beams. However, for a uniformly distributed load and a point load case the difference between the two buckling loads is considerable for short beams. Since all available design specifications provide solutions for lateral-torsional buckling only, these solutions are to be used with caution for short beams, as they may yield overestimated values of the buckling load for these two load cases. For these beams moment modification factors are calculated and compared with the provisions given in SSRC Guidelines. It is found that for relatively long beams, SSRC provisions give reasonably good estimation of moment modification factors but for short beams they provide overestimated results which may lead to overestimated calculation of the buckling capacity of the beam. Moment modification factors are dependent on the degree of beam mono-symmetry as well as on the span-to-depth ratio. For propped-cantilever beams, SSRC Guidelines always provide overestimated values of moment modification factors and the difference is too large for shorter beams. Therefore, while designing short beams, care must be taken for determining appropriate values of moment modification factors.

For long cantilever beams present results closely match with the experimental results of Kitipornchai et al. (1984). The effect of different types of bracing is investigated on

the buckling behavior of short and long monosymmetric I-beams. It is seen that top lateral bracings are very effective for beam sections having larger bottom flanges when a point load or a uniformly distributed load acts at the top flange and for the uniform moment case, except for the T-section or the inverted T-section cantilever beams. On the other hand, bottom lateral bracings are very effective for beam sections having larger top flanges. Simultaneously bracing both top and bottom flanges is definitely more effective. The bracing serves no purpose when the load acts at the bottom flange, except for inverted T-beams.

REFERENCES

ABAQUS/Standard User's Manual, Version 6.4, 2004 Hibbitt, Karlsson and Sorensen Inc, Pawtucket.

Bradford MA, Trahair NS, *Distortional buckling of I-beams*. Journal of Structural Division, ASCE, 1981; 107(ST2): 355-370.

Bradford MA., *Distortional Buckling of Monosymmetric I-Section Beams*. Journal of Construct. Steel Research, 1985; 5:123-136.

Bradford MA., *Buckling of Elastically Restrained Beams with Web Distortions*. Thin Walled Structures, 1988; 287-304.

Bradford MA., *Lateral-Distortional Buckling of Tee-Section Beams*. Thin Walled Structures, 1990; 10:13-30.

Bradford MA., *Buckling of Doubly-symmetric Cantilevers with Slender Webs*. Engineering Structures, 1992; Vol 14, No. 5, 327-334.

Bradford MA., *Elastic Buckling of Tee-section Cantilevers*. Thin Walled Structures, 1999; 33, 3-7.

Chajes A., *Principles of Structural Stability Theory*, Prentice-Hall 1974, New Jersey.

Galambos TV, *Guide to Stability Design Criteria for Metal Structures*. 4th Ed. 1988 John Wiley & Sons, Inc., New York.

Galambos TV, *Guide to Stability Design Criteria for Metal Structures*. 5th Ed., 1998 John Wiley & Sons, Inc., New York.

Goodier JN, *The buckling of Compressed bars by tension & flexure*. Bulletin 27, Dec. 1941; Cornell University Engineering Experimental Station.

Hancock GJ, Bradford MA and Trahair NS, *Web Distortion and Flexural Torsional Buckling*. Journal of Structural Division, ASCE 1980; 106(ST7):1557-1571.

Helwig TA, Frank KH and Yura JA, *Lateral-Torsional Buckling of Singly Symmetric I-Beams*. Journal of Structural Engineering, ASCE 1997; 123(9):1172-1179.

Hill HN, *Lateral Instability of Unsymmetrical I-beams*, Journal of Aeronautical Science, Vol. 9, Mar. 1942: 175.

Hughes O and Ma M, *Lateral-Distortional Buckling of Monosymmetric Beams under Point Load*. Journal of Structural Mechanics, ASCE 1996; 122 (10):1022-1029.

IS: 800-1984, *Indian Standard Code of Practice for General Construction in Steel* (Second Revision)

Johnson CP and Will KM, *Beam Buckling by Finite Element Procedure*, Journal of Structural Division. ASCE, 1974, 100(ST3): 669-685.

Kerensky OA, Flint AR and Brown WC, *The Basis for Design of Beams and Plate Girders in the revised British Standards* 153, Proceedings of Institution of Civil Engineers, Part III, Vol. 5, Aug. 1956: p. 396.

Kitipornchai S and Trahair NS, *Buckling Properties of Monosymmetric I-Beams*. Journal of Structural Division, ASCE 1980; 106(ST5):941-958.

Kiripornchai S, Dux FP and Richter JN, *Buckling and Bracing of Cantilevers*, Journal of Structural Engineering, ASCE, 1984; Vol 110 No.10: 2250-2262.

Kitipornchai S, Wang CM and Trahair NS, *Buckling of Monosymmetric I-Beams under Moment Gradient*. Journal of Structural Division, ASCE 1986; 112(4):781-799.

Load and Resistance Factor Design Specification for Highway Bridges, 1st Ed., 1994, American Association of State Highway and Transportation Officials (AASHTO), Washington, D.C.

Load and Resistance Factor Design, 2nd Ed., 1994, American Institute of Steel Construction, Chicago, Illinois.

Load and Resistance Factor Design Specification for Structural Steel Buildings, American Institute of Steel Construction's (AISC), 1999, Chicago, Illinois.

Loong-Hon Ng M and Ronagh HR, *An Analytical Solution for the Elastic Lateral Distortional Buckling of I-section Beams*. Advances in Structural Engineering 2004; Vol. 7 No. 2: 189-199.

Ma M and Hughes O, *Lateral-Distortional Buckling of Monosymmetric I-Beams under Distributed Vertical Load*. Thin Walled Structures 1996; 26(2):123-145.

Nethercot DA and Rockey K C, *A Unified Approach to the Elastic Lateral Buckling of Beams*, AISC Eng. J., Vol. 9, No. 3, 1972: 96-107.

Nethercot DA, *Elastic Lateral Buckling of Beams in Beams and Beam Columns: Stability and Strength* (ed. R. Narayanan), 1983, Applied Science Publishers, England.

O'Conner C, *The Buckling of Monosymmetric Beam Loaded in the Plane of Symmetry*, Australian Journal of Applied Science, Vol. 15, No. 4, Dec., 1964: p. 191.

Petterson O, *Combined Bending and Torsion of I-Beam of Monosymmetric Cross-section*, Bulletin No. 10, Dec., 1951 Division of Building Statistics and Structural Engineering, Royal Institute of Technology Stockholm Sweden.

Revised IS: 800, Draft for Revision of IS: 800-1984, Bureau of Indian Standards, 2003.

Timoshenko SP and Gere JM, *Theory of Elastic Stability*. McGraw Hill, New York, N. Y., 1961.

Wang CM and Kitipornchai S, *Buckling Capacities of Monosymmetric I-Beams*. Journal of Structural Engineering, ASCE 1986; 112(11):2373-2391.

Wang CM, Kiripornchai S and Thevendran V, *Buckling of Braced Monosymmetric Cantilevers*, International Journal of Mechanical Science, 1987, Vol 29, No. 5, 312-337.

Winter G, *Lateral Stability of Unsymmetrical I-beams and Trusses in Bending*, Proceedings, ASCE, Vol 67, No 10, Dec 1941: p. 1851.